



Schweizerische Eidgenossenschaft
Confédération suisse
Confederazione Svizzera
Confederaziun svizra

Département fédéral de l'environnement, des transports,
de l'énergie et de la communication DETEC
Office fédéral de l'énergie OFEN

Rapport annuel 2009

Dimensionnement des galeries et puits blindés

Design of steel lined pressure tunnels and shafts

Mandant:

Office fédéral de l'énergie OFEN
Programme de recherche Force hydraulique
CH-3003 Berne
www.bfe.admin.ch

Cofinancement:

Competence Center for Energy and Mobility CCEM-CH, CH-5232 Villigen PSI

Mandataire:

Ecole Polytechnique Fédérale de Lausanne EPFL
Laboratoire de Constructions Hydrauliques LCH
Station 18
CH-1015 Lausanne
lchwww.epfl.ch

Auteurs:

Fadi Hachem, EPFL-LCH, fadi.hachem@epfl.ch
Prof. Dr. Anton Schleiss, EPFL-LCH, anton.schleiss@epfl.ch

Responsable de domaine de l'OFEN: Dr. Michael Moser

Chef de programme de l'OFEN: Dr. Klaus Jorde

Numéro du contrat et du projet de l'OFEN: 154103 / 103095

L'auteur de ce rapport porte seul la responsabilité de son contenu et de ses conclusions.

Table of content

Sommaire	iii
1. Recall	1
2. Practical relevance of this research	1
3. State-of-the-art and gaps of knowledge	2
3.1 State-of-the-art	2
3.2 Remaining gaps of knowledge	2
4. An overview of the research plan and the main project objectives	3
5. Physical scaled model	4
6. Prototype measurements	6
7. Theoretical model	6
8. Project timetable	7
9. Follow-up of the project	8
10. Bibliography	8
11. Appendices	8

List of Figures

Figure 1.1 : Partners and main objectives of <i>HydroNet</i> project consortium	1
Figure 4.1 : Main objectives of the research project	4
Figure 5.1 : Scheme of the physical scaled model	5
Figure 5.2 : Detailed scheme of the test pipe and measuring sensors	5
Figure 6.1 : General plan view of <i>Grimsel II</i> power plant	6
Figure 7.1 : Cross section of the theoretical model of pressurized steel lined tunnels	7
Figure 8.1 : Project timetable schedule	7

Sommaire

La forte demande de l'énergie de pointe offre une occasion unique aux producteurs hydro-électriques suisses pour augmenter la capacité de production de leurs usines. Les centrales hydro-électriques doivent opérer à des vitesses variables assurant l'équilibre production-demande avec efficacité, flexibilité et sécurité. Par conséquent, les projets de pompage-turbinage ont gagné d'importance majeur car ils permettent un approvisionnement d'énergie de pointe en faisant circuler les eaux entre deux réservoirs amont et aval situés à des altitudes différentes.

Dans le but d'optimiser le comportement des aménagements hydro-électriques et plus particulièrement les aménagement de pompage-turbinage, un consortium technique nommé *HydroNet* a été mis en place pour définir une nouvelle méthodologie pour le dimensionnement, la fabrication, l'opération, l'auscultation et le contrôle des centrales hydro-électriques. Ce consortium permettra d'offrir de nouvelles idées à la technologie de production hydro-électrique et de maintenir la position privilégiée de la Suisse dans ce domaine ainsi que dans l'exportation de la haute technologie.

Le rôle clé de génie civil dans ce consortium se résume dans le dimensionnement, l'auscultation et le contrôle des galeries et puits blindés en se préoccupant essentiellement de la sécurité de ces ouvrages. La sécurité d'une centrale hydro-électrique est primordiale car ce type d'aménagement doit être dimensionner pour remplir son rôle pour une durée de service pas moins que 90 ans.

L'optimisation des règles de dimensionnement et la proposition de nouvelles méthodes de contrôle et d'auscultation des galeries et puits blindés constituent le sujet de cette thèse. Une attention particulière sera consacrée à l'interaction structure-fluide ainsi qu'à la propagation des ondes acoustiques dans l'eau et dans les roches avoisinantes. L'établissement et l'exploitation d'un modèle physique à échelle réduite ainsi que l'analyse des mesures effectuées sur prototype permettra d'établir des nouveaux modèles théoriques de l'interaction fluide-structure suite à des fluctuations de pressions provoquées par les coups de bâlier. Il sera ensuite possible de développer des nouvelles méthodes et procédures de dimensionnement pour les puits blindés. Ces méthodes seront basées sur le comportement contraintes-déformations du chemisage en acier en considérant l'interaction entre les différentes composantes de la structure à savoir; l'acier, le béton et le rocher. Les résultats de ces analyses représentent une cible cruciale en Suisse suite à la rupture du puits blindés de l'aménagement hydro-électrique de *Cleuson-Dixence* en décembre 2000. Une rupture provoquée par le développement et la propagation des micro-fissures dans les soudures de l'acier du blindage.

Depuis 1980, aucune recherche fondamentale n'a pas été menée dans le cadre de dimensionnement des puits blindés considérant l'interaction avec le rocher. Le comportement réel de la structure composée en acier, béton et rocher n'est pas encore totalement compris surtout l'effet des sévères coups de bâliers sur le comportement de la structure en court et long durée ainsi que sur la sécurité du blindage. A priori, des modèles en éléments finis existent actuellement mais ils ne sont pas calibrés dû à la déficit des données mesurées sur prototype. Ces mesures ne sont pas souvent disponibles, et si elles existent, elles sont inaccessibles pour les travaux de recherche.

Le dimensionnement et l'analyse de la sécurité des galeries et puits blindés basés sur l'idée de garder la contrainte admissible dans le blindage au-dessous de la limite

d'élasticité de l'acier utilisé sont devenus insuffisants depuis l'utilisation fréquente des aciers de blindage à haute résistance. Ce type d'acier possède un risque de rupture fragile plus élevé que les aciers ordinaires relativement ductiles.

Les études antérieures ont montré qu'il n'y a aucune raison pour s'inquiéter du problème de fatigue du blindage en aciers ductiles. Néanmoins, cette conclusion peut être critiquée quand l'acier à haute résistance est utilisé comme blindage pour les puits des aménagements hydro-électriques de haute chute et dans les centrales de pompage-turbinage. Dans ces dernières, les amplitudes des fluctuations de pression sont plus faibles mais possèdent une fréquence plus élevée conduisant ainsi à un nombre considérable de cycles de contrainte.

Ce projet de recherche vise à développer de nouvelles et innovatrices directives pour le dimensionnement des galeries et tunnels blindés. Elle traitera principalement, dans le cadre d'une thèse, les points suivants:

- 1- **Etude de littérature**, qui indiquera les paramètres principaux d'intérêt du problème et les pistes à conquérir.
- 2- **Bases théoriques**, dont le but principal est de décrire la physique derrière les différents phénomènes.
- 3- **Mesures sur prototype**, où le puits blindés d'une centrale électrique de pompage-turbinage sera équipé par des instruments de mesure non-intrusifs. Les résultats de ces mesures permettront de comprendre le comportement du blindage et de ses éléments principaux.
- 4- **Modélisation physique à échelle réduite**, d'une conduite en acier enrobée par du béton ou par d'autres matériaux. Des coups de bélier seront créés sous des conditions aux limites bien contrôlées et sous des opérations de vanne de fermeture bien définies.
- 5- **Analyse des mesures effectuées sur prototype**, qui seront utilisés pour vérifier les modèles théoriques et pour calibrer les modèles en éléments finis.
- 6- **Développement de modèle théorique**, basé sur l'analyse des résultats des essais décrivant la réponse de la structure à des pressions internes transitoires sévères.
- 7- **Nouvelles directives de dimensionnement**, pour le blindage des galeries et puits en acier à haute résistance soumis aux variations de pression hydrauliques internes sévères.
- 8- **Rapport de thèse et publications scientifiques**.

Ce rapport décrit brièvement les objectifs principaux de la thèse et résume les travaux effectués durant la période entre août 2008 et août 2009.

Mots clés : *Centrales hydro-électriques de pompage-turbinage, dimensionnement des puits blindés, structure composée, pression interne transitoire, mécanique de rupture fragile et fatigue, mesures sur prototype, propagation des ondes, directives de dimensionnement.*

1. Recall

Modern power plants are expected to operate at variable speed in a wide range of output power with improved efficiency, flexibility and safety. Therefore, the pumped storage power generation has gained in importance since it allows storing and generating electricity to supply high peak demands by moving water back and forth between reservoirs at different elevations.

A project consortium, called *HydroNet* (*Modern Methodologies for Design, Manufacturing and Operation of Pumped-Storage Power Plant*) (Figure 1.1) has been built aiming to converge towards a consistent standardized methodology for design, manufacturing, operation, monitoring and control of pumped storage power plants in order to give new impulsions in the hydropower technology and maintain the strong position of Switzerland in peak hydropower production as well as in the exportation of high valued technology.

One of the civil engineering field involved in this consortium is *the design and control of pressurized shafts and tunnels* with a special focus on safety. Since 1980's, no significant fundamental research has been performed aiming to integrate design with interaction between water, steel lining and rock mass. The results of these investigations stand for a crucial target in Switzerland since the collapse of the shallow buried pressure shaft of *Cleuson-Dixence* hydropower plant in December 2000.

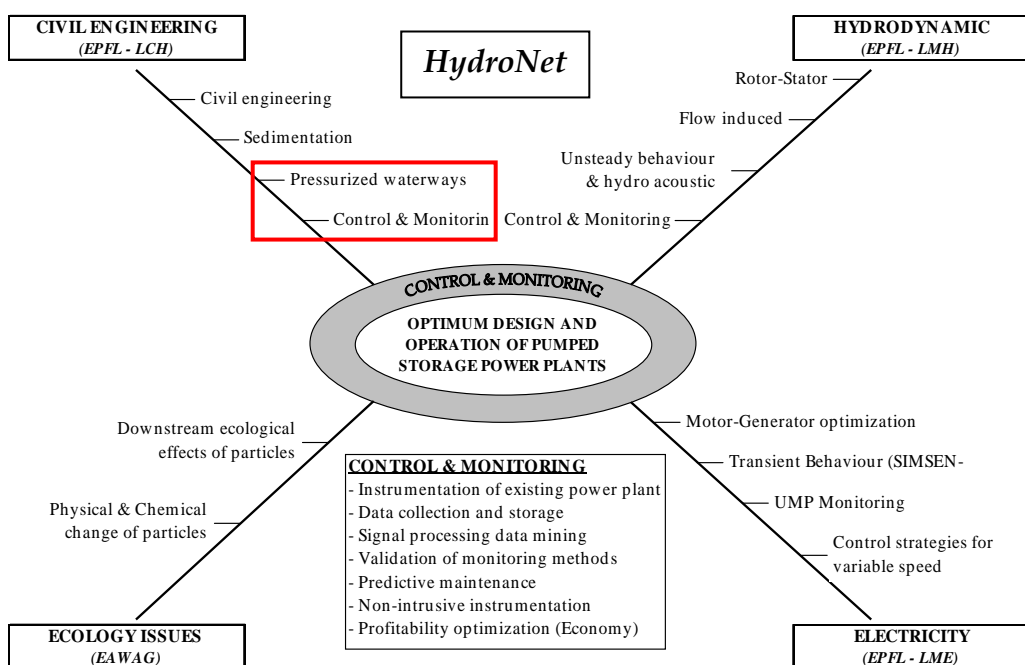


Figure 1.1 : Partners and main objectives of *HydroNet* project consortium

2. Practical relevance of this research

This research project will end to some practical applications, mainly:

- 1- **New design guidelines** for the steel tunnel liners using high-strength steel and subjected to severe internal hydraulic pressure fluctuations.
- 2- **Development of new theoretical model** based on the analysis of the test results describing the structure response during severe hydraulic transients.

3- **Relevant monitoring methods** for steel liner tunnels and shafts using non-intrusive instrumentation. These methods will detect some specific physical measurands needed to predict maintenance works that minimize the risk of a catastrophic failure of the structure.

3. State-of-the-art and gaps of knowledge

3.1 State-of-the-art

The *State-of-the-art*, has been already prepared based on an extensive literature review of the essential design requirements and fields related to the steel lining structure (refer to the "Demande de subside (2008)" Report addressed to *OFEN*). To understand the behaviour of such composite structure, a discussion has been done on the materials properties and the way that may influence the resistance of the structure. It was shown that the actual design is based upon the same concept of any composite structure where the need for a full understanding of the behaviour of its three composing materials: Steel, Concrete and Rock is essential for any attempt for design. It is known that the steel lining must carry loads without excessive yielding or rupture and that the geological and geotechnical parameters of the hosted rock are the key issue for determining the load sharing ratios between the composite materials of the steel lining system.

3.2 Remaining gaps of knowledge

Through an extensive literature study, a detail review of the available design rules for pressurized steel liner tunnels and shafts has shown that research and design has been conducted mainly during the period of construction of hydropower plant in Europe until the 1980's. Since then, no significant fundamental research has been performed aiming to integrate design with interaction between lining and rock mass.

The true behaviour of combined steel-concrete-rock linings is not yet fully understood, especially the influence of severe transient flow phenomena, such as water hammer effects, on the short and long term structural behaviour and safety of the lining.

The existing design methods have been based on the idea of keeping the allowable stress in steel liner below yielding point with respect to a certain requirements concerning properties of the steel used (e.g. ductility) and some construction details and tolerances to minimize stress raiser points. Designing and safety assessment of these structures based on the existing methods have become insufficient since recently very high strength steel liners are used with a high risk of brittle failure.

Previous studies have shown that there are no reason for concern with regard to the fatigue strength of the ductile steel linings. Nevertheless, this conclusion can be criticized when high-strength steel is used in high-head hydropower plant and in pumping-storage schemes where pressure waves of smaller amplitudes but of high frequencies can lead to a very high number of stress cycles.

It is well known that water hammer phenomenon forces the steel liner shell to vibrate. These vibrations create acoustic waves in water and pressure waves in the surrounding rock mass. These waves have not been measured before, even so, they can carry precious information about the response of the tunnel to transient pressure fluctuations. By

processing the measured wave signals, it is expected to assess the equivalent elastic properties of the steel lined tunnel or shaft.

The actual design criteria and methods for load sharing calculations for steel lined pressure tunnels and shaft, as well as, the actual gaps of knowledge have been reviewed and discussed in (Hachem and Schleiss, 2009). This paper is jointed to this report in Appendix A.1.

4. An overview of the research plan and the main project objectives

The research plan of this project has been submitted to the Director of the "Doctoral Program in Structures - EPFL" in the 8th of august 2008. It was accepted by the dean of the doctoral school of the EPFL in the 22nd of august 2008.

The hydraulic-mechanical interaction between water, steel, concrete and rock will be investigated in detail. This will allow better assessing of the technical potential of pressurized waterways to satisfy future practical applications of hydropower schemes submitted to severe market constraints, including multiple daily openings and closings manoeuvres in the power house due to peak load demands.

The research project mainly focus on the following subtasks :

- 1- **Literature study**, in which the available design rules for pressurized steel linings waterways and the coupled behaviour and load sharing calculation of the composite structure have been reviewed.
- 2- **Theoretical bases**, that may include theory on fracture mechanics of steel and fluid-structure interaction and wave propagation in water, in the steel liner and in the surrounding rock media. The main goal is to theoretically describe the main physics behind the different phenomena in question.
- 3- **Prototype measurements**, that will be performed on the pressurized shaft of *Grimsel II* power plant in Switzerland. The shaft will be equipped with non-intrusive instruments to acquire prototype measurements needed for calibration and verification of the theoretical model of the lining and its main elements.
- 4- **Physical scaled modelling**, which consists of a test conduit made of several pieces of different type of materials (steel, PVC and aluminium) where water hammer phenomenon will be created under controlled boundary conditions and gate operation. The propagation of pressure waves in water, in the pipe wall and through the pipe's cover will be measured and processed for different conduit layouts and configurations.
- 5- **Analysis of model and prototype measurements**, that will be used to verify theoretical developments and to calibrate finite element models.
- 6- **Development of theoretical model** based on the analysis of the test results describing the structure response during severe hydraulic transients.
- 7- **New design guidelines** for steel tunnel liners using high-strength steel and subjected to severe internal hydraulic pressure fluctuations.
- 8- **Dissertation report and scientific publications**

The main objectives of this research project are summarized in Figure 4.1.

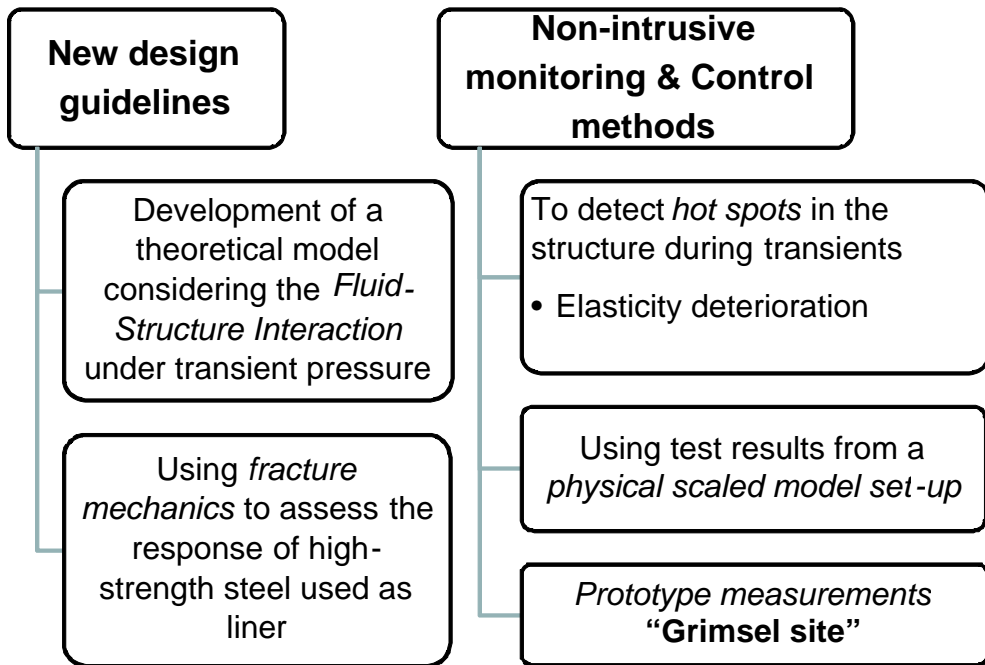


Figure 4.1 : Main objectives of the research project

5. Physical scaled model

In purpose to understand the complex problem related to waves propagation, a physical scaled model is now under construction (Figure 5.1). It will be equipped to be able to produce water hammer shock waves under a well controlled boundary conditions and gate operation.

In addition to the traditional physical measurements needed to study this type of problem (e.g. water flow, pressure transducers, etc.), the model will be equipped with two hydrophones and five geophones sensors that are able to capture pressure waves in water and waves propagating along and transmitted outward the pipe's wall and cover. The measured signals will be processed and studied in time and frequency domains trying to relate them to the elastic properties of the pipe.

Different configurations will be examined by changing systematically the position of the steel conduit flanges and by replacing and changing the position of conduit pieces made of other type of materials.

Figure 5.2 shows a more detailed view of the test pipe scheme. The construction drawings of the installation and the different test pipe configurations to be studied are given in Appendix A.2.

Tests will start by in the middle of September 2009 at the Laboratory of Hydraulic Machines (LMH) where the physical model is built. A total of about 40 to 45 configurations (see Appendix A.2) have to be tested and analyzed. The test campaign is expected to end in April 2010.

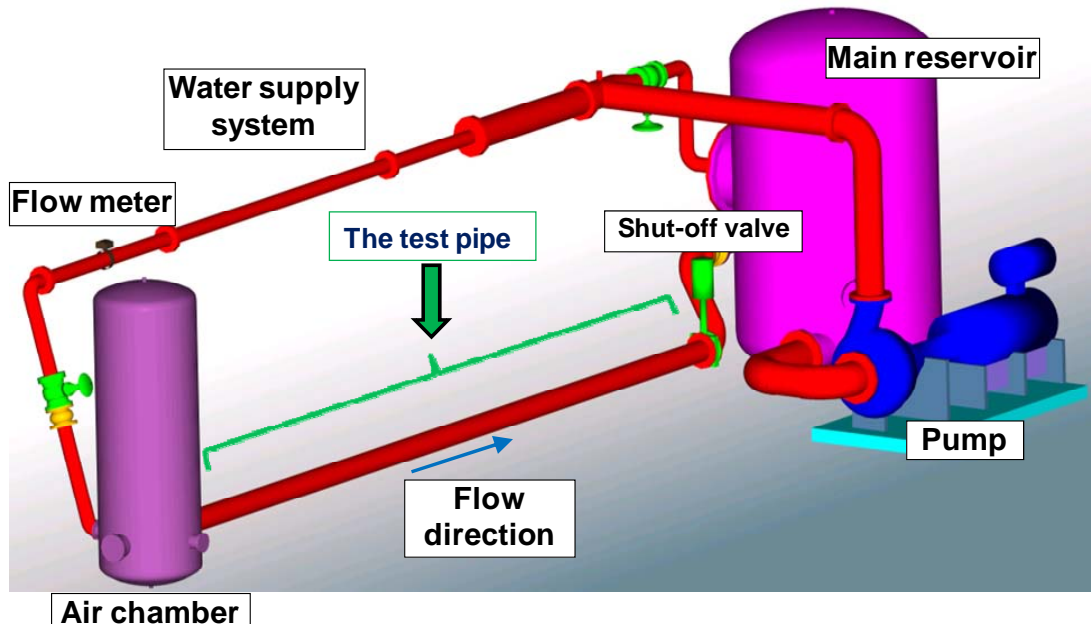


Figure 5.1 : Scheme of the physical scaled model

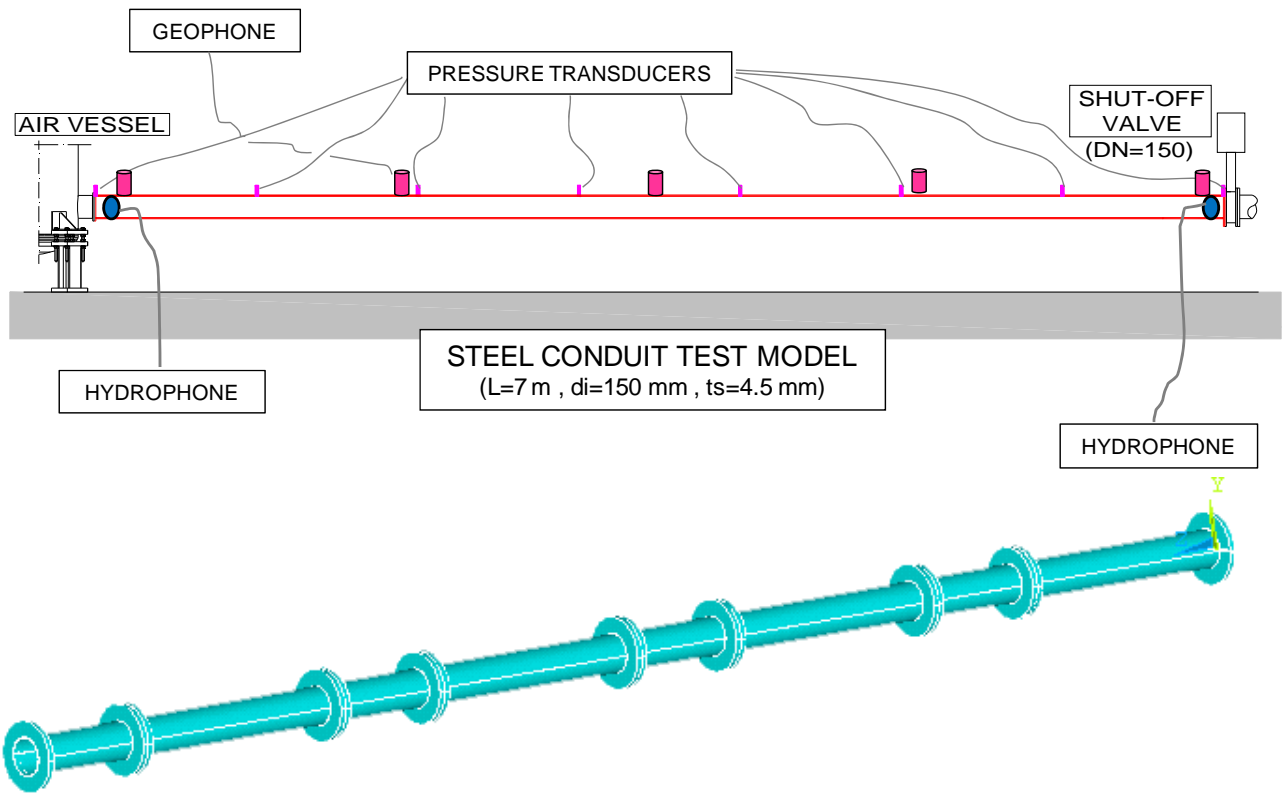


Figure 5.2 : Detailed scheme of the test pipe and measuring sensors

6. Prototype measurements

The pressurized shaft of the high-pressure side of the pumping-storage hydropower plant of *Grimsel II* in Switzerland (Figure 6.1) will be equipped with pressure sensors, geophones and hydrophones sensors allowing the performance of prototype-scaled measurements of the lining response and its main elements. Detailed analysis of results and comparison with the theoretical model will be performed to verify its adequacy and efficiency.

Based on the analysis of the test results, adaptation and optimization of the theoretical model will be performed to describe the coupled behaviour of water-steel-concrete and rock system during severe hydraulic transients.

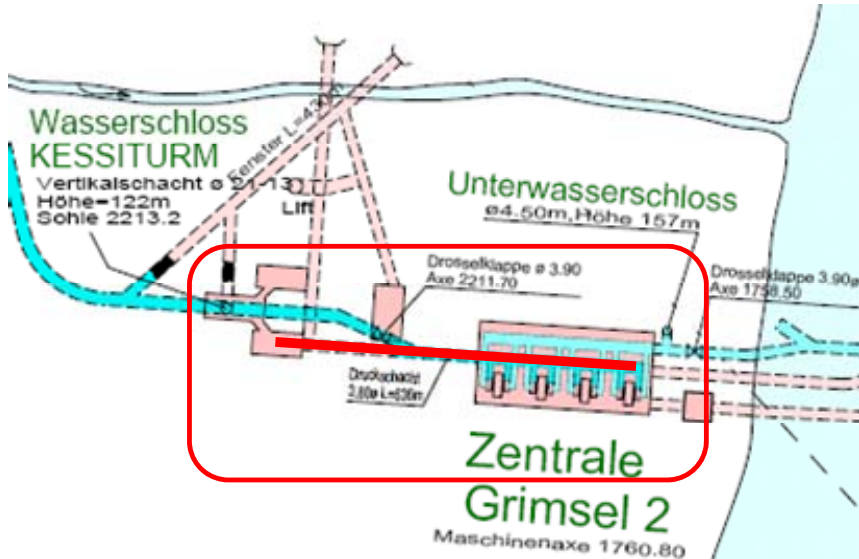


Figure 6.1 : General plan view of *Grimsel II* power plant

After several site investigations, the actual sensing equipments (position, performance, data acquisition system, etc.) have been identified and needs for other or more powerful equipments have been clarified (see Appendix A.3). The one-year measurement campaign is planned to start by the end of September 2009.

7. Theoretical model

A Fluid-Structure Interaction (*FSI*) theoretical model with axisymmetrical behaviour and longitudinal motion is actually under preparation (Figure 7.1). This model can detect the compressional water mode in water and the radial and axial propagation modes in the steel liner and in the far field rock zone.

The time-dependent stress diagrams, resulting from the *FSI* problem, will be used as input for the deterministic and probabilistic fracture mechanics models of steel liners. A finite element model will be build and results will be compared with those obtained from the theoretical model. The physical and prototype measurements will be used for calibration and verifications.

The final results may be used to adapt some existing design procedures in aeronautical field, nuclear power plants and long span steel bridges to steel liners design.

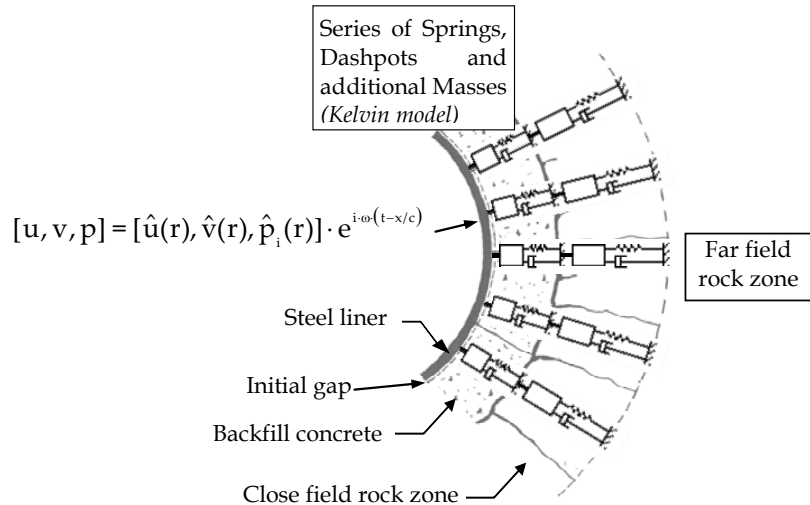


Figure 7.1 : Cross section of the theoretical model of pressurized steel lined tunnels

8. Project timetable

The time schedule of the different project phases can be given as follows :

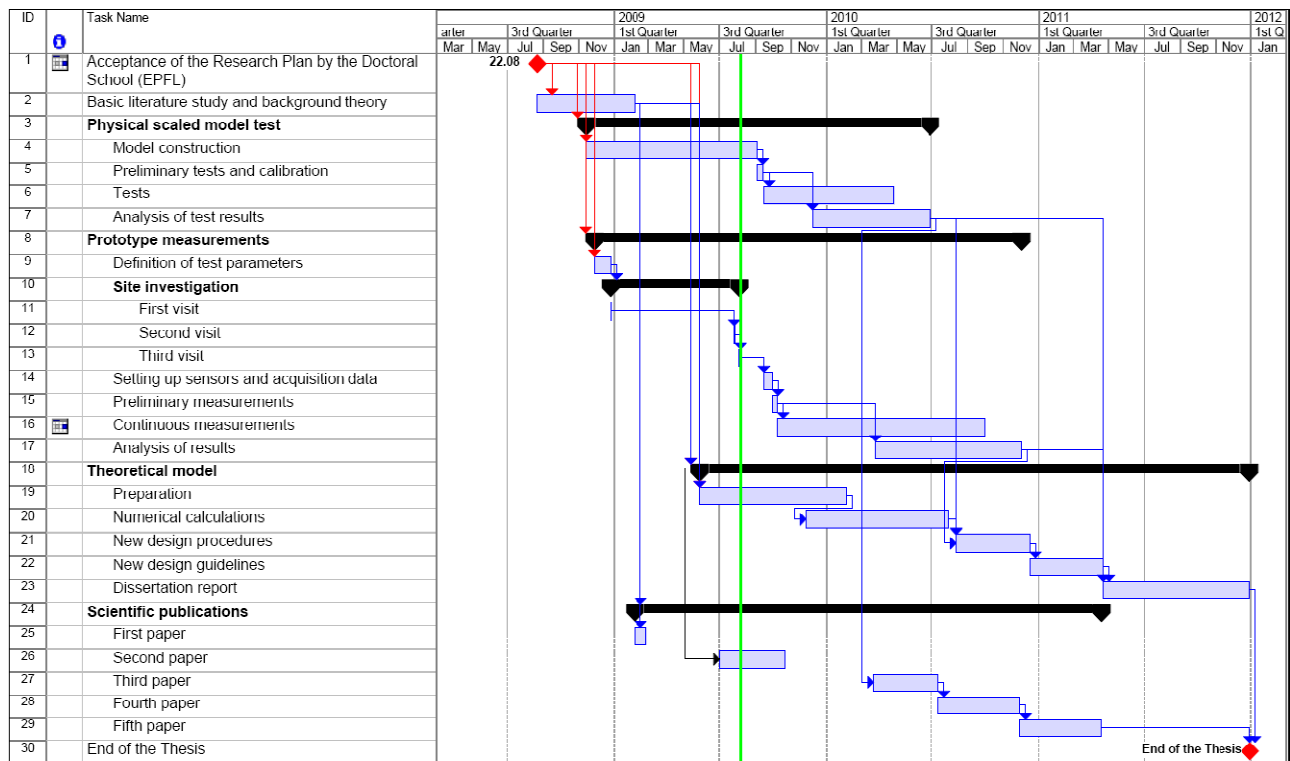


Figure 8.1 : Project timetable schedule

9. Follow-up of the project

Beside the following-up by the director of this research work, Prof. Anton Schleiss, this research project is supervised closely by the senior research associates, Dr Erik Bollaert and Dr Jean-Louis Boillat. Accordingly, progress meetings are planned regularly, every five to six weeks, with the research project director and the senior research associates.

One to two times a year, the progress state of the project will be presented as an internal conferences at LCH (one conference has been given on the 7th of November 2008 and the second will take place on the 4th of September 2009). Furthermore, two intermediate reports at the end of the first and the second year will be prepared (the first report has been submitted in August 2008).

In the framework of the multidisciplinary CCEM-project, periodical sessions (2 per year) will be organized to share information and to discuss the progress of the project (three technical meetings have took place until now).

10. Bibliography

Demande de subside à l'OFEN (2008). *Projet de recherche, Dimensionnement des galeries et puits blindés*. Laboratoire de Constructions Hydrauliques (LCH).

Hachem, F. and Schleiss, A. (2009). The design of steel-lined pressure tunnels and shafts. *International Journal on Hydropower & Dams*, 16(3):142-151.

11. Appendices

- A.1 The state-of-the-art of the design of steel-lined pressure tunnels and shafts.
- A.2 The construction drawings and test configurations of the physical scaled model.
- A.3 Sensing requirements for the prototype measurements.

A.1

The state-of-the-art of the design of steel-lined pressure tunnels and shafts

The design of steel-lined pressure tunnels and shafts

F. E. Hachem and A. J. Schleiss, Laboratory of Hydraulic Constructions, EPFL, Switzerland

The state-of-the-art of the design criteria and the methods for load sharing calculations for steel lined pressure tunnels and shafts is reviewed here. The design methods mainly based on allowable stresses in the steel liner can be questioned if high strength steel is used. After addressing the problematic nature of such steel, the author outlines the application of fracture mechanics theory in the design of steel liners. A new research project is briefly described, where the acoustic signal of waterhammer will be used to access the structural stiffness of steel lined pressure tunnels and shafts.

Steel-lined pressure shafts and tunnels in rock are the key structures of hydroelectric powerplants. Because of the higher peak energy demands, hydro plants have to operate under rough conditions as regards the output power with improved efficiency, flexibility and safety. Therefore, the development of new design guidelines for pressurized waterway systems is required, based on the detailed stress-strain behaviour of the lining, and taking into account a combination of different materials such as high strength steel, concrete and rock. The importance of such new guidelines has been underlined by the collapse of the shallow pressure shaft at the Cleuson-Dixence hydro plant in Switzerland, in December 2000.

Since the 1980s, no significant fundamental research has been carried out regarding the interaction between steel liners and the surrounding rock mass. The true behaviour of combined steel-concrete-rock linings is not yet fully understood, especially the influence of severe transient flow phenomena, such as waterhammer effects, on the short- and long-term structural behaviour and the safety of the lining. Powerful finite element models do exist, but they are rarely calibrated because of the lack of prototype measurements.

This paper gives an overview of existing methods for load sharing calculations and design guidelines for steel-lined pressure tunnels and shafts under internal water pressure. A distinction can be made between calculations for axisymmetrical isotropic and anisotropic rock masses surrounding the liner. High strength steel is more and more often used for steel liners. For such steel, design methods based on yielding strength can be questioned. Also, gaps in knowledge are identified and future research is suggested based on fracture mechanics theory, as well as the assessment of waterhammer-induced acoustic waves in water and pressure waves in the surrounding rock mass.

1. Current design criteria for steel liners

Basic criteria for the design of steel-lined sections of tunnels and shafts as recommended by Schleiss [1988¹] are:

- (A) working stress and deformation of the steel liner; and,
- (B) load-bearing capacity of the rock mass

Condition A

This refers to the behaviour of the steel liner, and includes:

- A1. stability of the steel liner under external water pressure;
- A2. limiting working stresses in the steel liner; and,
- A3. limiting local deformation of steel liner (crack bridging).

Condition A1

In accordance with normal practice, a factor of safety of 1.5 against buckling should be adopted. If the acting external water pressure is based, because of a lack of field data, on very conservative assumptions, a safety factor of between 1.15 and 1.30 is sufficient. In the case of a sandwich lining, the compressive stresses in inner concrete ring should be well below the ultimate strength of the concrete (the safety factors applied in the different codes vary from 1.8 to 2.5).

Condition A2

The stresses in the steel liner are derived based on the compatibility of the radial displacements of the steel and rock at their boundary, as transmitted by the backfill concrete. Load sharing between steel liner and rock should be determined by taking into account a cracked backfill concrete (no tangential stresses can be transmitted) and the effect of a crack stress-relieved rock zone.

Condition A3

The steel liner must be able to bridge any cracks in the backfill concrete which develop under internal pressure. Since, for reasons of symmetry, a minimum of two cracks will occur, the maximum expected width of the cracks will be equal to the half of the total circumferential deformation of the rock mass under internal pressure. This condition only comes into play for very thin steel liners as in case of sandwich linings with steel membranes where thickness are not governed by buckling.

Condition B

The purpose of this condition is, on the one hand, to check the load sharing assumed for Condition A2 and, on the other hand, to guarantee sufficient security against rock mass failure. The maximum rock mass participation is equal to the mechanical pressure developed at the boundary between the steel liner (or backfill concrete) and the rock at which the rock can no longer share the load. In principle, this limited load sharing is reached as soon as the maximum tensile stresses in the rock mass caused by that boundary pressure exceed the natural stresses in the rock mass (in a plan perpendicular to tunnel axis).

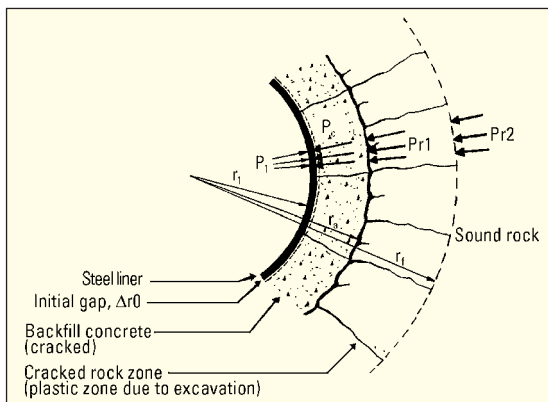


Fig. 1. Calculation model for steel liners with axisymmetrical behaviour.

In the following, the design criteria for internal water pressure are discussed more in detail.

2. Load sharing between the steel liner and surrounding rock mass

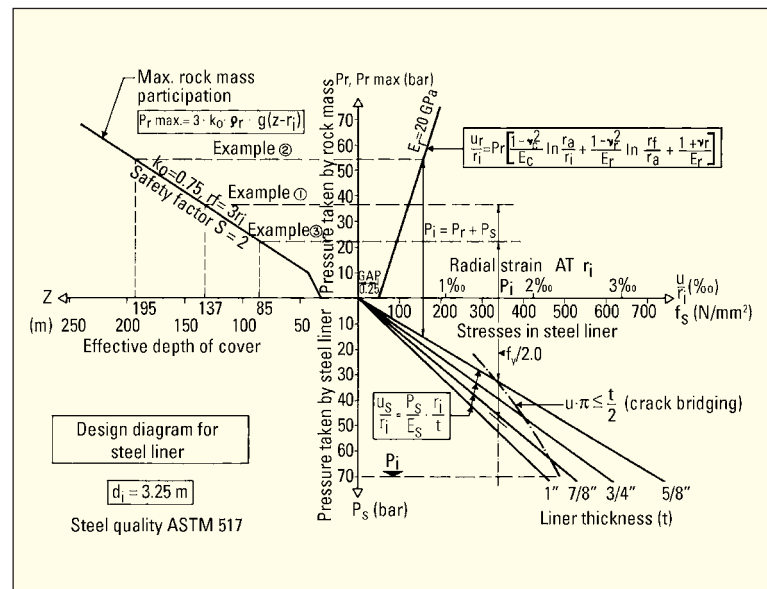
2.1 Radial symmetric calculation model

The determination of the load sharing between the steel lining, the backfill concrete and the surrounding rock mass is normally based on elastic theory. The radial deformation of the steel liner is put equal to the radial deformation of the backfill concrete and the rock mass in the so-called 'compatibility condition of deformations'.

For the calculation of the load sharing, five different zones are considered (see Fig. 1):

1. *Steel lining*, which is in direct contact with the pressurized water. It provides an impervious membrane and carries a certain part of the internal pressure p_i .
 2. *Initial gap*, between steel and backfill concrete. The steel liner will shrink as a result of the contact with cold water, leaving a small gap Δr_0 between the two materials. A typical value of Δr_0 equal to 0.25% of r_i is often used in design corresponding to a temperature decrease of 20°C. The gap caused by the shrinkage of the backfill concrete is normally filled by grouting before the pressure shaft or tunnel is put into operation.
 3. *Concrete*, as a backfill between the steel liner and the excavated rock. Having a tensile strength of about 1 to 2 MPa, the backfill concrete is normally fissured under internal pressure and cannot transmit tangential stresses.

4. *Cracked rock zone*, which corresponds to the disturbed part of the rock mass as a result of excavation methods and of the change in the stress field around tunnel. Being cracked, this part of the rock mass cannot transfer tensile stresses. The external radius r_f and the modulus of elasticity E_{cm} for this disturbed zone are the two most important parameters to be determined for the design. The external radius r_f of the disturbed rock is normally estimated at between one and five times the excavated tunnel radius r_a [Brekke and Ripley, 1987²]. Nishida *et al.* [1982³] have shown that for mechanical excavation by tunnel boring machine (TBM), r_f was roughly 0.3 m, and for excavation by drill and blast, r_f was roughly 0.5 to 1.3 m, both measured in 5 m diameter tunnel in crystalline rock. Therefore, for good rock conditions, values of r_f higher than 1.0 to 1.5 times r_a are considered as very conservative. Schleiss [1988¹] suggested 0.5 to 1.0 m for tunnels excavated by (TBM) and 1.0 to 2.0 m for drill and blast.



5. *Sound rock zone*. This non-disturbed zone is assumed as a homogeneous, isotropic and elastic material having a mean elastic deformation modulus E_{cm} that can be measured in-situ or estimated for example by the Hoek-Brown method [Hoek, 2006⁴] or by *RMR* or *Q* indexes [Bieniawski, 1973⁵] and [Gurocak *et al.*, 2007⁶].

Fig. 2. Seeber design diagram including maximum rock mass participation criterion [Schleiss, 1988¹].

2.2 Solving the compatibility condition

2.2.1 Analytical methods

On the basis of the compatibility of deformations, Table 1 illustrates approaches for the calculation of the load transfer suggested by various authors. The main differences between these approaches arise from assumptions regarding the backfill concrete (cracked or uncracked), the extension of the disturbed rock zone as well as the annular gap.

The effect on the rock mass participation and the presence of an annular gap can change the results significantly. For example, increasing the outer radius of the disturbed rock zone from $2r_a$ to $5r_a$ decreases the percentage of the load transferred to rock from 45 to 20 per cent. Decreasing the modulus of elasticity of the disturbed rock mass, having an outer radius of $3r_a$, from 75 to 50 per cent of E_{cm} decreases the load transferred percentage from 40 to 35 per cent.

2.2.2 Graphical methods

Several authors have developed graphs for the design of steel liners [Nicolopoulous, 1983⁷].

Seeber [1975⁸] suggested a graphical solution of the compatibility condition of deformations at the steel-rock interface. Its application is illustrated in the lower pressure tunnel of the North Fork Stanislaus river hydroelectric project. In this project, Schleiss [1988¹] enhanced Seeber-diagram to take into account the rock confinement and the crack bridging criteria in isotropic rock mass. Once the internal water pressure has been fitted between the working line of the rock mass (upper right quadrant of Fig. 2) and the working line of the steel liner (lower right quadrant), the strain and hoop stress in the steel liner can be obtained directly as well as the load sharing between the steel liner and the concrete-rock system.

The required effective depth of cover (upper left quadrant) and the crack bridging criteria (lower right quadrant) will be discussed later.

Table 1 : Load transfer calculation techniques for tunnel steel linings under internal pressures

Reference	Steel	Backfill concrete	Cracked rock zone	Steel-Concrete-Rock system	Remarks
Täche [1949 ³²]	$(p_s, r_i^2)/(E_s, t) \cdot (1-v^2)$	$(p_c, r_c)/E_c \cdot (1-v_c^2) \cdot \ln(r_a/r_c)$	$[(p_c, r_c)/E_m] \cdot (1-v_s^2) \cdot \ln(r_i/r_a)$	+	Annual gap, Δr_θ
Brekke [1987 ²] after Gunmensky and Chu (1948)	$(p_s, r_i^2)/(E_s, t)$	Treated as intact rock	Treated as intact rock	$[(p_c, r_c)/E_m] \cdot (1+v_s)$	Not considered
Vaughn [1956 ³³]	$(p_c, r^2)/(E_s, t)$	$(p_c, r_c)/E_c \cdot (1-v_c^2) \cdot \ln(r_a/r_c)$	$[(p_c, r_c)/E_m] \cdot (1-v_r^2) \cdot \ln(r_i/r_a)$	$[(p_c, r_c)/E_m] \cdot (1+v_s)$	Not considered
Brekke [1987 ²] after Patterson et al (1955)	$(p_s, r_i^2)/(E_s, t)$	$(p_c, r_c)/E_c \cdot (1-v_c^2) \cdot (2r_a)$	$(p_c, r_c)/E_m \cdot (1-r_i^2/r_a^2) \cdot (2r_a r_i)$	$[(p_c, r_c)/E_m] \cdot (1+v_r)$	0.0003, r_i
Brekke [1987 ²] after Moody (1959)	$(p_c, r_i^2)/(E_s, t)$	$(p_c + p_d) \cdot (r_a, r_c) / (2 \cdot E_c)$	Treated as intact rock	$[(p_c, r_c)/E_m] \cdot (1+v_r)$	Considered but formulated
Brekke [1987 ²] after Laufer and Seeber [1961 ²⁰]	$(p_s, r_i^2)/(E_s, t) \cdot (1-v^2)$	Treated as intact rock	Treated as intact rock	$[(p_c, r_c)/E_m] \cdot (1+v_r)$	0.0003, r_i
Brekke [1987 ²] after Ramos and Abrams (1968)	$(p_c, r^2)/(E_s, t)$	Treated as disturbed rock	$[(p_c, r_c)/E_m] \cdot \ln(r_i/r_a)$	$[(p_c, r_c)/E_m] \cdot (1+v_s)$	0.0002, r_i
Brekke [1987 ²] after Kruse (1970)	$(p_s, r_i^2)/(E_s, t) \cdot (1-v_s^2)$	$[(p_c, r_c)/E_c] \cdot \ln(r_a/r_c)$	$[(p_c, r_c)/E_m] \cdot \ln(r_i/r_a)$	$[(p_c, r_c)/E_m] \cdot (1+v_r)$	0.0001, r_i
Brekke [1987 ²] after Jacobsen (1977)	$(p_s, r^2)/(E_s, t) \cdot (1-v_s^2)$	Treated as intact rock	$[(p_c, r_c)/E_m] \cdot \ln(r_i/r_a)$	$[(p_c, r_c)/E_m] \cdot (1+v_s)$	-
Schleiss [1988 ¹]	$(p_s, r_i^2)/(E_s, t)$	$[(p_c, r_c)/E_c] \cdot (1-v_c^2) \cdot \ln(r_a/r_c)$	$[(p_c, r_c)/E_m] \cdot (1-v_r^2) \cdot \ln(r_i/r_a)$	$[(p_c, r_c)/E_m] \cdot (1+v_s)$	0.0005, r_i
Moore [1989 ³⁴]	$(p_s, r_i^2)/(E_s, t) \cdot (1-v_s^2)$	$[(p_c, r_c)/E_c] \cdot \ln(r_a/r_c)$	$[(p_c, r_c)/E_m] \cdot \ln(r_i/r_a)$	$[(p_c, r_c)/E_m] \cdot (1+v_r)$	0.0025, r_i
EM 1110-2-2901 [1997 ¹⁸]	$(p_s, r_i^2)/(E_s, t) \cdot (1-v_s^2)$	$[(p_c, r_c)/E_c] \cdot \ln(r_a/r_c)$	$[(p_c, r_c)/E_m] \cdot \ln(r_i/r_a)$	$[(p_c, r_c)/E_m] \cdot (1+v_s)$	$r_i \cdot \Delta T$; and it is nil in tropical and semi-tropical of E_m [Eskilsson, 1999 ³⁵]
				$[(p_c, r_c)/E_m] \cdot (1+v_r)$	$r_i \cdot \Delta T$

2.2.3 Numerical methods

If the rock behaviour is anisotropic and inhomogeneous around the tunnel, analytical solutions are not available anymore and numerical methods as finite element approaches have to be used.

2.3 Anisotropic rock mass behaviour

If the behaviour of the rock mass is anisotropic (for example, bedding, foliation, jointing, and so on) the circumferential stresses in the steel liners can vary considerably. A rough estimation is often used for axisymmetrical rock mass behaviour by using an overall rock mass stiffness equal to the minimum value that the rock can have [Brekke and Ripley, 1987²]. Nevertheless, with such an approach, the non-axisymmetrical deformation of the steel liner is not taken into account.

Eristov [1967⁹ and 1968¹⁰] has studied the behaviour of pressure tunnel linings in anisotropic, orthotropic elastic media by dividing the lining into n beam elements. He established an analytical system that gives the total radial deformation at θ angle, $\Delta r(\theta)$, along the liner perimeter as a function of the internal pressure, the steel liner characteristics and the elastic reaction coefficients of the rock mass k_x and k_y ($k_x < k_y$) measured in two perpendicular directions x and y . A relationship has been also given to estimate the reaction coefficients of the rock mass in the θ direction.

These relationships can be written, according to Fig. 3, as follows:

$$\Delta r(\theta) = \frac{p_i \cdot r_i^2}{E_s \cdot t} - \frac{k_x \cdot \Delta r_x \cdot r_i^2}{E_s \cdot t} + p_\theta \frac{3r_i^2}{E_s \cdot t^2} \left(\frac{4}{\pi} - \theta \sin(\theta) - \cos(\theta) \right) \quad \dots [2.1]$$

where: $p_\theta = (k_\theta \cdot \Delta r(\theta) - k_x \cdot \Delta r_x) \Delta S$... [2.2]

$$k_\theta = \frac{k_x \cdot k_y}{k_x \cdot \sin^2(\theta) + k_y \cdot \cos^2(\theta)} \quad \dots [2.3]$$

$$\Delta S = \frac{2\pi r_i}{n} \quad \dots [2.4]$$

and n is the number of beam elements of the steel liner having the length of ΔS .

It should be mentioned that Eristov's method is similar to the Finite Element Analysis described in US Army Manual [1997¹¹]. In this Manual, the radial and tangential spring stiffnesses (elastic reaction coefficients) are estimated, for a 2-D calculation model, from equations (2.5) and (2.6).

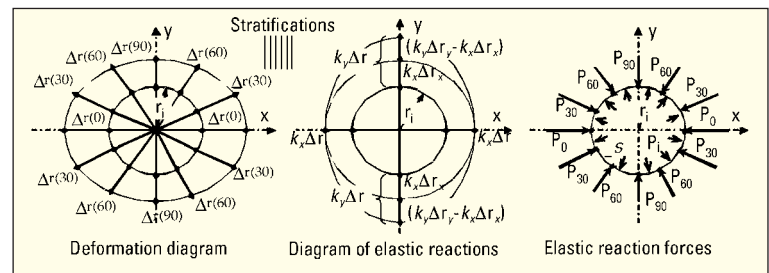
$$k_\theta = \frac{E_{rm}(\theta) \cdot \alpha}{1 + \nu_r} \quad \dots [2.5]$$

$$k_{t\theta} = k_\theta \frac{G_{rm}(\theta)}{E_{rm}(\theta)} = 0.5 \frac{k_\theta}{1 + \nu_r} \quad \dots [2.6]$$

where α is the arc defining the beam elements, in radians:

3. Assessment of the maximum rock mass participation

The calculation techniques solving the compatibility condition for load transfer assume directly a full load sharing with the rock. Therefore, the question is for which minimum rock cover full load sharing can be admitted.



It is clear that for a tunnel or shaft situated very close to the ground surface or to the underground caverns and chambers, the steel lining has to be designed for full internal pressures without taking into account load transfer to the rock. For regions with low rock cover, the capacity of the rock mass to withstand the pressures transmitted from the steel lining is usually determined by in-situ stress measurements (hydraulic jacking or fracturing and overcoring). Often, when the rock cover is below $20r_i$ [Schleiss, 1988¹ and 1992²] no load sharing is considered. In the Indian Standards [1996¹³], no load sharing is taken into account if the overburden weight is less than 40 per cent vertically and 120 per cent horizontally compared with the internal water pressure under normal loading conditions.

The left hand side of Fig. 2 shows the maximum rock mass participation curve calculated by Schleiss as a function of overburden rock. This curve has been implemented in the design diagram for the lower pressure tunnel of the North Fork Stanislaus river hydroelectric project. A safety factor of $SF = 2.0$ was used.

In assessing adequate confinement, most of the designers use static head considering only the upsurge water levels in the surge tank. The best way to assess the maximum rock mass participation is to measure in-situ rock stresses in boreholes near the future tunnel or shaft. Since such measurements are not always available, the rock mass participation can be estimated from overburden as the Fig. 2. Nevertheless, an assumption of the ratio between the minimum horizontal stress and the overburden has to be made (k_0 value).

It has to be noted that the minimum primary stress can be lower than the one caused by the overburden measured perpendicular to the rock surface for steep slopes [Seeber, 1985¹⁴]. When measuring the perpendicular distance to the rock surface, protruding ridges and noses do not affect the stress in the rock masses in a valley side, and should therefore be neglected. Simplified topographic maps with smooth contour lines, drawn inside such protruding features, should be drawn [Broch, 1984¹⁵].

4. Crack bridging

Seeber [1975⁸] proposed a crack bridging criteria since the liner must be able to bridge the cracks in the backfill concrete. In the most critical case, only two cracks can occur in the backfill concrete. To bridge these cracks safely, Seeber stated that the steel wall thickness must be at least equal or higher than the crack width in a stratified rock mass having distinct elasticity modulus in both directions, parallel and perpendicular to stratifications. So, the crack bridging criteria without considering a safety factor, was defined by:

$$t \geq 2u_s \Rightarrow \frac{u_s}{r_i} \leq \frac{t}{2r_i} \quad \dots [4.1]$$

where u_s is the radial deformation and r_i the internal radius of the liner.

Fig. 3. Calculation model according to Eristov (1967, 1968) for steel liners in anisotropic rock mass. At left: non-axisymmetric deformation of steel liner, in the middle: elastic reactions of the steel liner and at right: elastic reaction forces between steel liner and rock.

According to Schleiss [1988¹], for isotropic behaviour of the rock mass, the deformation u_s leads to a uniform increase of the steel liner perimeter. For a safety factor equal to 2.0, the crack bridging criteria becomes:

$$t \geq 2\pi u_s \Rightarrow \frac{u_s}{r_i} \leq \frac{t}{2\pi r_i} \quad \dots [4.2]$$

In the lower right quadrant of Fig. 2, this crack bridging criteria is implemented in the design diagram.

For a detailed assessment of the crack bridging criteria, Seeber and Danzl [1988¹⁶] defined a critical ratio $(d_f \max / t)_{crit}$, where $d_f \max$ is the width of the largest crack in backfill concrete, taking into consideration the properties of steel, the friction coefficient between steel liner and concrete, μ_{sc} as well as, the internal pressure and the internal radius to steel thickness ratio (r_i/t) . They proposed a relationship for $(d_f \max / t)_{crit}$ in anisotropic stratified rocks as follows:

$$(d_f \max / t)_{crit} = 2 \frac{u_s}{t} \quad \dots [4.3]$$

where:

$$\frac{u_s}{r_i} = 0.5 \frac{\varepsilon_m}{1 - \varepsilon_m} \frac{1}{\mu_{sc}} \ln \left(\frac{f_y \cdot p_i \frac{r_i}{t}}{f_m \cdot p_i \frac{r_i}{t}} \right) \quad \dots [4.4]$$

and, f_m and ε_m are respectively the maximum strength and the corresponding strain of steel used.

5. Comparison of recommendations and codes for the design of steel liners

5.1 Loads and load combinations

In Europe, the C.E.C.T. [1980¹⁷] recommendations have been developed for the design and construction of steel-lined tunnels and shafts. The US Army Manuals [1995¹¹ and 1997¹⁸] give recommendations for design of permanent steel linings. The Indian Standards [1996¹³] treat

the subject of the structure design of steel lining.

For the design of penstocks and steel lined tunnels, the allowable stress method is used in which all loads (both dead and live loads) have a load factor equal to 1. Loads include:

- *Construction loads* (handling, erecting, and so on)
- *Live loads* (earthquake)
- *Dead loads* (weight of the structure and rock loads)
- *Intermittent loads* (filling and drainage of tunnel)
- *Service loads* that are divided to:

- (1) Maximum static head minus the head losses plus the waterhammer and surge during load rejection when all units are operating with normal governor closure time
- (2) Minimum static head minus the waterhammer and down surge occurring when all units operate from speed no load to full load acceptance
- (3) The head at transient maximum surge.

- *Emergency loads* which include:

- (1) Maximum static head plus waterhammer and surge during partial gate closure in critical time of $(2L/a)$ seconds at maximum rate with the cushioning stroke being inoperative in one unit
- (2) Same as No1 but with the cushioning stroke being inoperative in all units.

- *Exceptional loads* including:

- (1) Unforeseen operation that produce instantaneous changes in the flow rate
- (2) Rapid closure of turbine gates in less than $(2L/a)$ seconds for maximum flow rate
- (3) Rhythmic opening and closing of the turbine gates when complete cycle of gate operation is performed in $(4L/a)$ seconds.

The combinations of loads adopted by different recommendations are given in Table 2.

The waterhammer or overpressure calculated by the elastic water column theory [Parmakian, 1963¹⁹ and Jaeger, 1977²⁰], is in general assumed to be linearly distributed along the developed length of the shaft, between the connection point of the shaft with the surge tank or with the water intake and the nearest downstream closing gate.

Table 2: Loads and load combinations (normal, intermittent, emergency and exceptional) for steel lining design, according to the three recommendations: CECT [1980], USACE Manual [1995] and Indian standards [1996]

Loads	Loading combinations							
	Normal			Intermittent		Emergency	Exceptional	
Construction	X						X	
Live							X	
Dead	X	X	X	X	X	X	X	X
Intermittent				X	X	X		
Service No. 1		X						
Service No. 2			X					
Service No. 3				X				
Emergency No. 1						X		
Emergency No. 2						X		
Exceptional No. 1							X	
Exceptional No. 2								X
Exceptional No. 3								X
Considered in the recommendation								
C.E.C.T.	O	O	O	O	O	O	O	O
EM 1110-2-3001	O	O	O	O	O	O	O	O
Indian Standards	O		O	O	O	O	O	O

5.2 Equivalent and allowable stresses in steel liners

According to C.E.C.T. [1980¹⁷] and as general rule, steel stresses are divided into primary and secondary stresses. The primary stresses induced deformations increase with the loads even after the yield strength is exceeded. Secondary stresses are local stresses where deformation stop to increases with forces when the elastic limit of the material used is reached. For circumferential or tangential stresses in steel liner, primary stresses are those caused by the internal pressure taking into consideration the initial gap and the resistance of the hosted rock, if it is considered. In longitudinal direction, primary stresses occur as a result of Poisson's effect of the circumferential stresses and caused by friction.

According to C.E.C.T. [1980¹⁷], at least for primary stresses, all calculations have to be made in the elastic range. The equivalent stress in the steel, σ_{eq} is evaluated after combining longitudinal and circumferential stresses with the Hencky-Von Mises theory in triaxial state of stresses according to the relationship:

$$\sigma_{eq} = \sqrt{0.5(\sigma_{s1} - \sigma_{s2})^2 + 0.5(\sigma_{s2} - \sigma_{s3})^2 + 0.5(\sigma_{s3} - \sigma_{s1})^2} \quad \dots [5.1]$$

In plane stress condition ($\sigma_{s3} = 0$), Eq. (6.1) becomes:

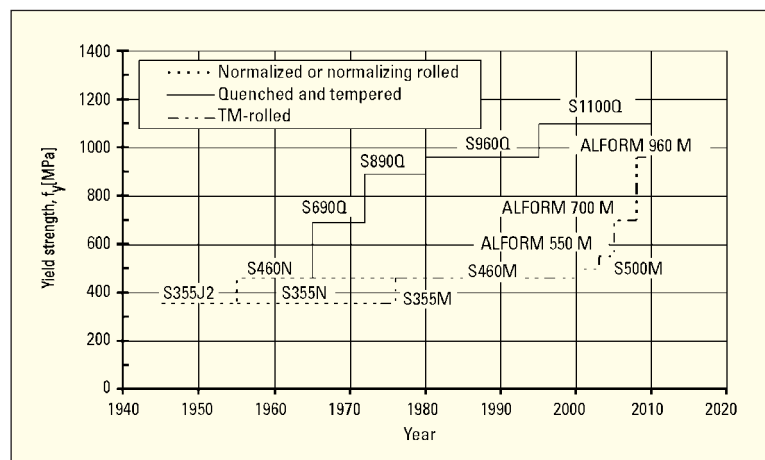
$$\sigma_{eq} = \sqrt{\sigma_{s1}^2 - \sigma_{s1}\sigma_{s2} + \sigma_{s2}^2} \quad \dots [5.2]$$

The equivalent stress should not be higher than the allowable stress at any point of the steel liner. In Table 3, ratios of the allowable steel stresses to yield or tensile strengths as recommended in different sources are given. It can be noticed that for each load combination, these ratios are different if the internal pressure is shared or not with the rock mass.

6. Problematic nature of high strength steel

6.1 Historical development of the steel strength

The development of new steel grades was always driven by the demand of having optimal mechanical characteristics for different uses. To increase the yield strength of steel, alloying carbon and manganese has some adverse effects on the weldability of the steel. A second possibility is the heat treatment where fine-grained structure is obtained with a better toughness.



An updated version of the historical context of rolled steel products taken from [Samuelsson and Schröter, 2005²¹] is shown in Fig. 4.

Until 1950, steel which is today known as S355 J2 according to EN 10025, was considered as a high strength steel. From the 1960s, the application of the 'Quenching and Tempering' process for steel grades began. Today, this process gives steel grades with yielding strength up to 1100 MPa and more, although only grades up to 960 MPa yield stress are standardized. In the 1970s, the 'Thermo-Mechanical rolling process was developed. This process produces grades up to 960 MPa with better welding performance than steels produced by (QT).

Fig. 4. Historical development of yield strength for rolled steel products.

6.2 Requirement for yield to tensile strength ratio

Most of the design codes define an upper limit of the yield to tensile strength ratio. Normally, the yield strength considered in the design should not be higher than 80 per cent (for steel plates thicker than 50 mm) and than 90 per cent (for thinner steel plates) of the tensile strength. This limitation penalizes the use of high strength steels in structural applications. It has been shown that this limitation is not relevant because the toughness is independent of the yield to tensile strength ratio [Langenberg et al., 2000²²].

6.3 Ductility and toughness

The toughness is the ability of a material to absorb energy prior to fracture. The larger the area under the stress-strain curve, the tougher the material is. In general, the toughness decreases with increasing yield strength of steels.

Table 3: Allowable stresses in terms of what is used by some organizations and codes

Organization standard	Reference	Load combination											
		Normal				Intermittent				Emergency		Exceptional	
		Without rock mass participation	With rock mass participation	Without rock mass participation	With rock mass participation	Without rock mass participation	With rock mass participation	Without rock mass participation	With rock mass participation	Without rock mass participation	With rock mass participation	Without rock mass participation	With rock mass participation
		%f _y	%f _u										
AISI	Brekke after AISI	100	67										
C.E.C.T.	C.E.C.T. (1980)	91		50		100						68-100	56
PG&E	Brekke after PGE	100	67	67	33								
SCE	Brekke after SCE												
USACE	EM 1110-2-3001	50	25			67	33			100	50		
USBR	Brekke after USACE	100	67										
Indian Standards	IS (1995)	60	33	90	67	67	40	100		90	60	100	100

High toughness and low carbon equivalent values in ductile steel allow for lower welding preheat temperatures, which in turn, result in less hardening and reduced tendency of cold cracking.

6.4 Hydrogen induced cracking

The cold cracking or delayed cracking is one of the most common and serious problems encountered in weldings of high strength steel. It can occur in the heat affected zone (HAZ) and in fusion zone (FZ) of the weldings. Tests have shown that hydrogen absorption can reach 7 ml/100 g under welding without using shielding materials (for example inert and semi-inert gases, blanket of granular fusible flux of limes, silica and so on). It can be reduced to 2 ml/100 g by using suitable shielding materials.

Fig. 5. Calculation results of an example using the traditional and the fracture mechanics design approach. The upper figure shows the variation of the required steel liner thickness and the weight of steel liner as a function of the yield strength of the steel. The lower figure depicts the variation of the allowable tensile steel against the yield strength. Example's inputs are: $pi = 18 \text{ MPa}$, $ri = 1.9 \text{ m}$, Safety Factors against yielding and against brittle fracture = 2.0, $ac = 25.4 \text{ mm}$ and $ac/2c = 0.2$

6.5 Corrosion and stress corrosion cracking

In the presence of oxygen and water, or under certain soil and electrical conditions, refined iron tends to return to its more stable form, iron oxide (rust). This reversion is an electrochemical natural process inherent to steel [AWWA, 2004²³].

Tensile stresses, cyclic stresses or high frequency vibrations acting combined with a corrosive environment can enhance or accelerate the deterioration of steel known as the phenomenon of stress corrosion cracking. For high strength steel, the stress corrosion cracking is a sort of weakening caused by hydrogen penetrating into cracks and diffusing from the crack tips toward the material. The origin of this hydrogen can be H_2 gas molecules, water or dissociated H_2S molecules. The hydrogen interacts with the micro-fracture facilitating there initiation and propagation. High strength steels and their welds are sensitive to such phenomenon in presence of water and humidity.

6.6 Fatigue loading and fatigue process

Fluctuations of internal pressures and potential structural vibrations of the steel liner are considered as fatigue loading. The consequence is time variation of the working stresses in the structure. Fatigue failures are avoided by ensuring that all critical features, such as longitudinal weldings of the steel liner, have an adequate fatigue strength. The most widely method used at the design stage, is based on the plot of stress (S) against the number of cycles to failure (N), which is known as an $S-N$ curve for the relevant detail class of the weldings [Maddox, 1991²⁴].

Tagwerker [1980²⁵] has studied pressure oscillations in the power conduits of three hydropower stations producing peak-load. Based on a number of load cycles up to 1000 cycles per year, and for ductile steel liners with a yield strength equal to 520 MPa, it was concluded that such oscillating loads are of no concern regarding fatigue strength of the linings. Nevertheless, Seeber [1985²⁴ and 1985²⁶] pointed out that it was not the somewhat higher static internal water pressures caused by surge tank oscillation which was the problem in some peak-load hydro plants, but rather the high frequency of the dynamic water pressures caused by waterhammer with smaller amplitudes.

It is also known that the fatigue strengths of welded details are independent of the tensile properties of the steel. As a consequence, the $S-N$ design curves are also common to high strength steels welded satisfactorily.

In fact, the validity of $S-N$ curves for high strength steel was explained by Maddox [1991²⁴] and Barsom and Rolfe [1999²⁷] in referring to the initiation and propagation of fatigue cracks. It was observed that the tensile strength of steel has little effect on the rate of propagation of a crack. Unwelded specimens show a benefit from increases in tensile strength as a result of the existence of crack initiation, or incubation periods in addition to that required for propagation. On the contrary, welded specimens have a constant fatigue strength, determined essentially by the propagation phenomenon alone. Such behaviour is related to the presence of pre-existing crack like flaws, such as hydrogen inherent intrusions, for which in fact, crack initiation has been achieved.

Welded high strength steel, therefore, offers no intrinsic advantage in term of fatigue strength. On the contrary, there may be a higher number of potential cracks and flaws in the welds. The risk of having cracks that propagate beyond the critical size is therefore higher.

6.7 Corrosion fatigue

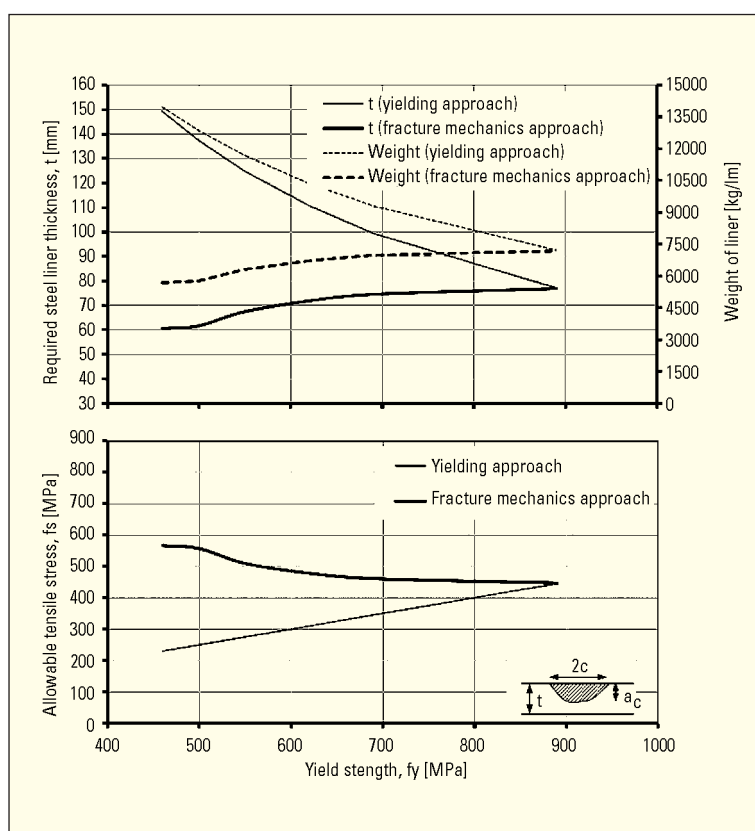
The fatigue design rules are normally based on the test data obtained in dry air at ambient temperature. Therefore, they do not consider corrosion which may have a significant influence on allowable fatigue stresses.

In fact, cracks accelerate corrosive attack. If the fluctuating stresses are high enough to propagate fatigue cracks from stress concentrations, corrosive reactions may accelerate their growth. Thus, the corrosion fatigue strength of a welded joint can be smaller than that under dry conditions. Furthermore, localized corrosive attack at stress concentrations and surface defects can increase the severity of the stress concentration and produce fatigue cracks.

7. Application of fracture mechanics theory to the steel liner design

7.1 The deterministic approach

In an unflawed member, the traditional design of a steel structure under tensile stresses is based on the



criteria of preventing yielding by keeping the driving stress σ_{eq} below the resistance stress f_y . Accordingly, for structures containing initial cracks, the stress intensity factor, K_I is a calculated driving factor which must be kept below the resistance factor K_{IC} to prevent brittle fracture.

For steel liners, crack-like defects are often present but designers normally assume that, if a steel of sufficient ductility is used, local yielding occurs and redistributes stresses in the vicinity of stress raisers. This local yielding may not occur in high strength steel and therefore, the risk of a brittle failure will increase. Crack-like defects are normally considered in modern design when high strength steel is used in the structure of nuclear powerplants, long span steel bridges and in the aeronautical industry. The selection of materials and allowable stress levels is based on the fact that discontinuities may be present or may initiate and propagate under cyclic loads or stress corrosion cracking. Therefore, cracks size can reach a critical value where K_I becomes larger than K_{IC} producing the brittle failure of the steel.

The use of high strength steel liner using thick welded plates in hydropower plants together with the increase of the dynamic pressures, lead to a higher risk of potential cracks in the steel liner welds and thus, an increasing of the risk of brittle failure.

To illustrate the use of the fracture mechanics theory for selecting an appropriate material for the steel liner, the calculation results of an example [Barsom and Rolfe, 1999²⁷] are given in Fig. 5. An internal pressure of 180 bars and a liner radius of 1.9 m are assumed. No load sharing with the surrounding rock is considered. The safety factor against yielding and brittle fracture of 2.0 is considered. An external surface flaw with a depth a_c equal to 25.4 mm and a depth to length ratio of 0.2 is assumed as the maximum crack size that could not be detected and repaired during steel liner inspections. The minimum steel liner thickness for handling purposes is considered equal to 25.4 mm.

The results show that the required steel liner thickness using the fracture mechanics theory increases with the increase of the yielding strength of the steel. For the same theory, the allowable tensile stress, f_s decreases when the yielding strength increases. Fig. 5 shows that for steel yield strength higher than 900 MPa and for steels with relatively low values of K_{IC} , the fracture mechanics theory becomes critical when fracture is a possible mode of failure.

7.2 The probabilistic approach

The residual dispersion with random distributions of lattice defects in steel plates and welds confirm the random nature of such material damages. Thus, a probabilistic rather than a deterministic approach should be used in the modern design of steel liners.

Probabilistic Fracture Mechanics (PFM) is well developed in the nuclear and aeronautical industries [Besuner and Tetelman, 1977²⁸; Provan, 1987²⁹; Nicholson and Ni, 1997³⁰]. It should be also applied to steel liners of pressure tunnels built with welded high strength steel and loaded by high dynamic pressure fluctuations with high number of stress cycles.

The keystone of the PFM approach is a deterministic engineering model of one or more system failure modes combined with assumed or proposed statistical variations of controlling parameters expressed as cumulative Probability Distribution Functions (PDF). The basis of PFM is the simple axiom that a given mode of failure event (E) will occur when the stress

σ_w associated with the failure mode exceeds the mode governing strength σ_f . The probability of failure according to mode (E) is given by:

$$P(E) = P(Y < 0) = PDF(y = 0) \quad \dots [7.1]$$

where the strength margin Y is:

$$Y = \sigma_f - \sigma_w = G(x_i) \quad \dots [7.2]$$

with $i = 1, \dots, n_x$, depends on input variables (of number n_x) that affect component stress or strength or both, and G is a concise deterministic summary of all prior engineering experience, models and assumptions. The x_i are the values of the controlling parameters described as a random variables X_i with cumulative distribution functions assumed to be known and represented by:

$$PDF(x_i) = P(X_i \leq x_i) \quad \dots [7.3]$$

The solution of equations (7.2) and (7.3) to obtain $PDF(Y)$ in Eq. (7.1) may be done in closed-form for simple cases or by using numerical solution, such as the Monte-Carlo (MC) simulation, if the $PDF(x_i)$ and $G(x_i)$ distributions are complicated.

If it is assumed that the equivalent stress σ_{eq} , the yielding strength f_y and the brittle fracture strength f_f of a steel liner can be represented by normal distribution curves [Besuner and Tetelman, 1977²⁷ after Osgood], failure occurs by the yielding mode (E_y) ($Y_y = f_y - \sigma_{eq} < 0$) or by the fracture mode (E_f) ($Y_f = f_f - \sigma_w < 0$) when the distribution curves overlap. This approach considers, for a given crack, that variations in f_f occur from variations in the steel fracture toughness, K_{IC} and in the depth of the critical crack, a_c according to equation:

$$f_f = \frac{K_{IC}}{\sqrt{\pi a_c}} \quad \dots [7.4]$$

Another approach [Nicholson and Ni, 1997³⁰] considers statistically varying crack length, orientation and number. The crack length is described by a two-parameter probability density function (Gamma distribution), the crack orientation is described by a uniform distribution and the crack number by a binomial distribution. Fracture mechanics is combined with extreme value probability theory (for example, order statistics) to produce extreme value distribution for strength depending on the expected number of cracks in the steel liner, the parameters of the mode of the fracture model and the parameters of the crack length distribution.

8. Remaining gaps in knowledge

The existing design methods for steel liner are based on the concept of allowable stress below yielding strength. Using steel with high ductility combined with some construction details and tolerances have been considered as a safe design minimizing stress raiser points. Nevertheless, this design concept is not appropriate if very high strength steel is used having a high risk of brittle failure. Schleiss [2002³¹] pointed out that the design criteria, outlined in section 1, have to be adapted in the case of high risk of failure with catastrophic consequences.

For ductile steel liners, experience has shown that in view of dynamic pressures caused by waterhammer, the issue of fatigue strength is not critical.

Nevertheless, if high strength steel is used under conditions with severe waterhammer pressure of high frequencies and very high number of stress cycles, as occur in pumped-storage plants, fatigue strength can become an issue.

Waterhammer produces a sound inside steel liners due to vibration. These acoustic waves in the water are also transmitted by pressure waves into the surrounding rock mass. They can carry valuable information about the response of the tunnel to dynamic pressures. By analysing the measured wave signals, the equivalent elastic properties of the steel lined tunnel or shaft may be assessed.

9. Outlook for future research

In the framework of the HydroNet project (Modern methodologies for the design, manufacturing and operation of pumped storage plants), the design criteria for steel liners will be enhanced to take into account new tendencies such as high strength steel and high dynamic loadings. The signal processing of acoustic waves propagating inside the steel liner and the surrounding will be used to obtain valuable information about the modification of the local elastic properties of the structure.

To verify the enhanced design concept, prototype measurements will be carried out on a pumped-storage plant in Switzerland. The steel-lined pressure shaft will be equipped with hydrophones placed at various locations. The measured acoustic wave signals will then be linked to the stiffness of the system.

The acoustic wave response of the structural stiffness of a system will be experimentally studied. The goals are to link pressure and acoustic signals inside a conduit to the pressure wave signal measured at the outer surface of the lining and to detect the amplitude and the location of a changed stiffness from transient pressure measurements at defined locations.

The experimental set-up consists of a steel pipe supplied with pressurized water. A shut-off valve can generate transient flow conditions with a closure time of less than one second. The pipe will be divided into several reaches with different wall stiffnesses.

The pressure fluctuations at the various measurement sections of the test pipe will be measured. The measurement sections will also be equipped with geophones. At the downstream end of the conduit pipe a hydrophone sensor will be provided for the acquisition of acoustic plane waves in water generated by the pressure fluctuations and pipe wall vibrations. The measured signals will be processed and studied in time and frequency domains using the Fast Fourier and Wavelets transforms.

This methodology should allow for the structural safety of steel lined pressure and shafts to be assessed in the future with non-intrusive measurements during operation. ◊

Acknowledgments

The study is part of the research project HydroNet (Modern methodologies for the design, manufacturing and operation of pumped storage plants) funded by the Swiss Competence Center Energy and Mobility (CCEM-CH), the Swiss Electric Research and the Swiss Office for Energy.

References

1. Schleiss, A., "Design criteria applied for the Lower Pressure Tunnel of the North Fork Stanislaus River Hydroelectric Project in California". *Rock Mechanics and Rock Engineering*, Vol. 21, No. 3, 1988.
2. Brekke, T. and Ripley, B., "Design strategies for pressure tunnels and shafts". Technical Report, University of California, Berkeley, USA; 1987.
3. Nishida, T., Matsumura, Y., Miyamoto, Y., and Hori, M. (1982). "Rock mechanical viewpoint on excavation of pressure tunnel by Tunnel Boring Machine". In International Symposium on Rock Mechanics, Aachen; May 1982.
4. Hoek, E., "Practical rock engineering." Course Notes, University of Toronto, Canada; 2006
5. Bierniawski, Z., "Engineering classification of jointed rock mass". Technical Report; *Civil Engineers*, Vol. 15, No. 12; 1973.
6. Gurocak, Z., Solanki, P., and Zaman, M. M., "Empirical and numerical analyses of support requirements for a diversion tunnel at the Boztepe dam site, eastern Turkey", *Engineering Geology*, Vol. 91, Nos. 2-4; 2007.
7. Nicolopoulos, A., "Current design procedures for steel-lined pressure tunnels", *Canadian Journal of Civil Engineering*, 10 (1, Mar. 1983):150-161; 1983.
8. Seeber, G., "Neue Entwicklungen für Druckstollen und Druckschächte". *Österreichische Ingenieur-Zeitschrift*, 18(5):140-149. 1975.
9. Eristov, V. S., "Experimental studies of pressure tunnel linings in anisotropic formations", *Gidrotekhnicheskoe Stroitel'stvo*, 12:19-21. 1967.
10. Eristov, V. S., "Computation of pressure tunnel linings in anisotropic rocks", *Hydrotechnical Construction*, Vol. 1, No. 5; 1968.
11. US Army Manual, Planning and design of hydroelectric power plant structures (EM 1110-2-3001), US Army Corps of Engineers; 1995.
12. Schleiss, A., "Erforderliche Felsüberdeckung bei Druckstollen und Druckschächten", *Wasser, Energie, Luft*, No. 11/12, 1992..
13. Indian Standards, "Indian Standard, Code of practice for design of tunnels conveying water (Division 14)", Bureau of Indian Standards; 1996.
14. Seeber, G., "Power conduits for high-head plants (Part one)", *Water Power & Dam Construction*, June 1985.
15. Broch, E., "Unlined high pressure in areas of complex topography", *Water Power & Dam Construction*, Vol. 36 No. 11; 1984.
16. Seeber, G. and Danzl, K. "Zur Bemessung von Druckschachtpanzerungen auf Innendruckbelastung", *Österreichische Ingenieur-Zeitschrift*, Vol. 133, No.4; 1988.
17. C.E.C.T., "Recommendations for the design, manufacture and erection of steel penstocks of welded construction for hydroelectric installations". European Committee of Boiler, Vessel and Pipe work Manufacturers; 1980
18. US Army Corps of Engineers, Tunnels and shafts in rock US Army Manual, (EM 1110-2-2901), 1997..
19. Parmakian, J., "Waterhammer analysis", Dover Publications, Inc., New York, USA; 1963.
20. Jaeger, C., "Fluid Transients in Hydro-Electric Engineering Practice", Glasgow and London, UK; 1977.
21. Samuelsson, A. and Schröter, F., "High-performance steels in Europe", Technical Report; 2005.
22. Langenberg, P., Niessen, T., and Dahl, W., "Bruch- und Verformungsverhalten von hochfesten Stählen mit Streckgrenzen von 690 bis 890 MPa", *Stahlbau*, Vol. 69, 2000.
23. AWWA, "External corrosion – Introduction to chemistry and control, Manual of water supply practices" (M27, 2004). American Water Works Association, Denver, CO, USA; 2004.
24. Maddox, S., "Fatigue strength of welded structures. Abington publishing, Second edition; 1991.
25. Tagwerker, J., "The frequency of surge tank oscillations and their effect on the fatigue resistance of tunnel liners", *Österreichische Wasserwirtschaft*, Vol. 32 (5-6 May-June 1980).
26. Seeber, G., "Power conduits for high-head plants (Part two)", *Water Power & Dam Construction*; July 1985
27. Barsom, J. and Rolfe, S., "Fracture and fatigue control in structures: Applications of fracture mechanics. ASTM, Butterworth-Heinemann, West Conshohocken, Third edition; 1999.
28. Besuner, P.M. and Tetelman, A.S. "Probabilistic fracture mechanics", *Nuclear Engineering and Design*, Vol. 43, No. 1, 1977.
29. Provan, J., "Probabilistic fracture mechanics and reliability". Martinus nijhoff publishers, Quebec, Canada; 1987.
30. Nicholson, D.W. and Ni, P., "Extreme value probabilistic theory for mixed-mode brittle fracture", *Engineering Fracture Mechanics*, Vol. 58, Nos. 1-2); 1997..

31. **Schleiss, A.**, "Berücksichtigung des Restrisikos bei der Konzeption und Bemessung von hochbeanspruchten Druckschächten". In Int. Symposium Moderne Methoden und Konzepte im Wasserbau, Versuchsanstalt für Wasserbau, Hydrologie und Glaziologie (VAW), VAW-Mitteilung No. 175; 2002.

32. **Tâche, J.** (1949). Contribution à la théorie et au calcul du blindage d'une galerie circulaire. Bulletin Technique Vevey, (1):19-27.

33. **Vaughan, E.W.**, "Steel linings for pressure shafts in solid rock". In: Proceedings, American Society of Civil Engineers; 1956.

34. **Moore, E. T.**, "Design of steel tunnel liners", Technical Report, Proceedings, International Conference on Hydropower, New York, USA; 1989.

35. **Eskilsson, J. N.**, "Design of pressure tunnels", Geotechnical Special Publication, Vol. 90; 1999.

Notations

a = pressure wave velocity of waterhammer, (m/s)
 a_c = depth of the critical crack in the steel liner, (m)
 c = half-length of the critical crack in steel liner, (m)
 $d_{f\max}$ = width of the biggest crack in backfill concrete, (m)
 E_c = elasticity modulus of backfill concrete, (MPa)
 E_r = in-situ rock modulus, (MPa)
 E_s = elasticity modulus of steel liner, (MPa)
 E_{crm} = elasticity modulus of cracked rock zone, (MPa)
 E_{rm} = elasticity modulus of sound rock mass, (MPa)
 f_i = steel brittle fracture strength, (MPa)
 f_m = steel maximum strength, (MPa)
 f_s = allowable stress in steel tunnel liner, (MPa)
 f_u = steel tensile strength, (MPa)
 f_y = steel yield strength, (MPa)
 k_0 = ratio of the minimum horizontal to vertical in-situ stresses, (-)
 k_θ = radial reaction coefficient of rock at θ coordinate (Eristov method), (MPa)
 $k_{t\theta}$ = tangential reaction coefficient of rock at θ coordinate (Eristov method), (MPa)
 K_{IC} = steel fracture toughness, (MPa.m^{0.5}) or (ksi.in^{0.5})
 K_I = stress intensity factor, (MPa.m^{0.5}) or (ksi.in^{0.5})
 k_p = ratio of plastic to elastic deformation of rock, (-)
 k_x = reaction coefficient of rock mass in x direction, (MPa)
 k_y = reaction coefficient of rock mass in y direction, (MPa)
 L = developed length of tunnel between surge tank and gates, (m)
 n = number of beam elements of the steel liner, (-)
 p_c = uniform pressure transmitted to concrete applied at radius r_c , (MPa)
 p_i = internal water pressure, (MPa)
 p_r = pressure taken by the concrete-rock system, (MPa)
 p_{r1} = uniform pressure transmitted to cracked rock zone at radius r_a , (MPa)
 p_{r2} = uniform pressure transmitted to sound rock zone at radius r_s , (MPa)
 p_s = pressure taken by the steel liner, (MPa)
 p_θ = elastic reaction forces of rock mass in θ direction (Eristov method), (MN)
 r = radius measured from tunnel axis, (m)
 r_a = inner radius of cracked rock zone, (m)
 r_c = inner radius of backfill concrete, (m)
 r_s = inner radius of the sound rock zone, (m)
 r_t = inner tunnel radius, (m)
 t = steel liner thickness, (m)
 u_s = radial deformation of the steel liner, (m)
 u_r = radial deformation of the rock mass, (m)
 z = depth of the tunnel below surface, (m)
 a = arc defining the beam elements (Eristov method), (radian)
 Δr_0 = initial gap between steel liner and concrete, (m)
 $\Delta r(\theta)$ = radial deformation at θ angle (Eristov method), (m)
 Δr_x = rock mass deformation in the x direction (Eristov method), (m)
 Δr_y = rock mass deformation in the y direction (Eristov method), (m)
 ΔS = beam element length of the steel liner (Eristov method), (m)
 ΔT = temperature variation of the steel liner, (°C)
 μ_{sc} = friction between steel and concrete, (-)
 v_c = Poisson's ratio of backfill concrete, (-)
 v_r = Poisson's ratio of the rock mass, (-)
 v_s = Poisson's ratio of steel, (-)
 ω = thermal coefficient of expansion of steel, (°C⁻¹)
 ρ_r = unit mass of rock, (kg/m³)
 σ_{eq} = equivalent stress in steel liner (Hencky-Von Mises stress), (MPa)
 σ_{s1} = tangential steel stress in liner, (MPa)
 σ_{s2} = radial steel stress in liner, (MPa)
 σ_{s3} = longitudinal steel stress in liner, (MPa)
 σ_{tm} = tensile strength of the rock mass, (MPa)
 θ = polar angle coordinate, (°)
 ε_m = steel deformation at f_m , (-)



F. Hachem



A. Schleiss

Fadi Hachem is a Civil Engineer who graduated in 1999 from the Lebanese University, and holds a Master of Advanced Studies in Hydraulic Engineering from the Ecole Polytechnique Fédérale de Lausanne (EPFL). He is currently a research assistant in the Laboratory of Hydraulic Constructions (LCH-EPFL). During his nine years of professional experience, he worked on several projects in the field of Hydraulic Structures for water supply and hydropower schemes, flood protection and feasibility studies. He has been involved in executive design and rehabilitation studies for projects in Lebanon (design studies for RCC and rockfill dams), in Switzerland (Hydroelectric and flood protection projects) and in Algeria (feasibility studies for water supply schemes).

Prof. Dr. Anton J. Schleiss graduated in Civil Engineering from the Swiss Federal Institute of Technology (ETH) in Zurich, Switzerland, in 1978. After joining the Laboratory of Hydraulic, Hydrology and Glaciology at ETH as a Research Associate and Senior Assistant, he obtained a Doctorate of Technical Sciences on the subject of pressure tunnel design in 1986. After that he worked for 11 years for Electrowatt Engineering Ltd, in Zurich and was involved in the design of many hydropower projects around the world as an expert on hydraulic engineering and underground waterways. Until 1996 he was Head of the Hydraulic Structures Section in the Hydropower Department at Electrowatt. In 1997 he was nominated full professor and became Director of the Laboratory of Hydraulic Constructions (LCH) in the Civil Engineering Department of the Swiss Federal Institute of Technology Lausanne (EPFL). The LCH activities comprise education, research and services in the field of both fundamental and applied hydraulics and design of hydraulic structures and schemes. The research studies and expertise involve both numerical and physical modelling. At present eleven PhD projects are ongoing at LCH under his guidance. Prof. Schleiss is also Director of the Master of Advanced Studies (MAS) in Hydraulic Engineering held in Lausanne in collaboration with ETH Zurich and the universities of Innsbruck (Austria), Munich (Germany), Grenoble (France) and Liège (Belgium). He is also involved as an international expert in several dam and hydropower plant projects all over the world as well as flood protection projects mainly in Switzerland. Since April 2006 he has been Director of the Civil Engineering program of EPFL. His is chairman of the Swiss Committee on Dams (SwissCOLD).

Laboratory of Hydraulic Constructions (LCH), Ecole polytechnique fédérale de Lausanne (EPFL), Station 18, CH-1015 Lausanne, Switzerland.

A.2

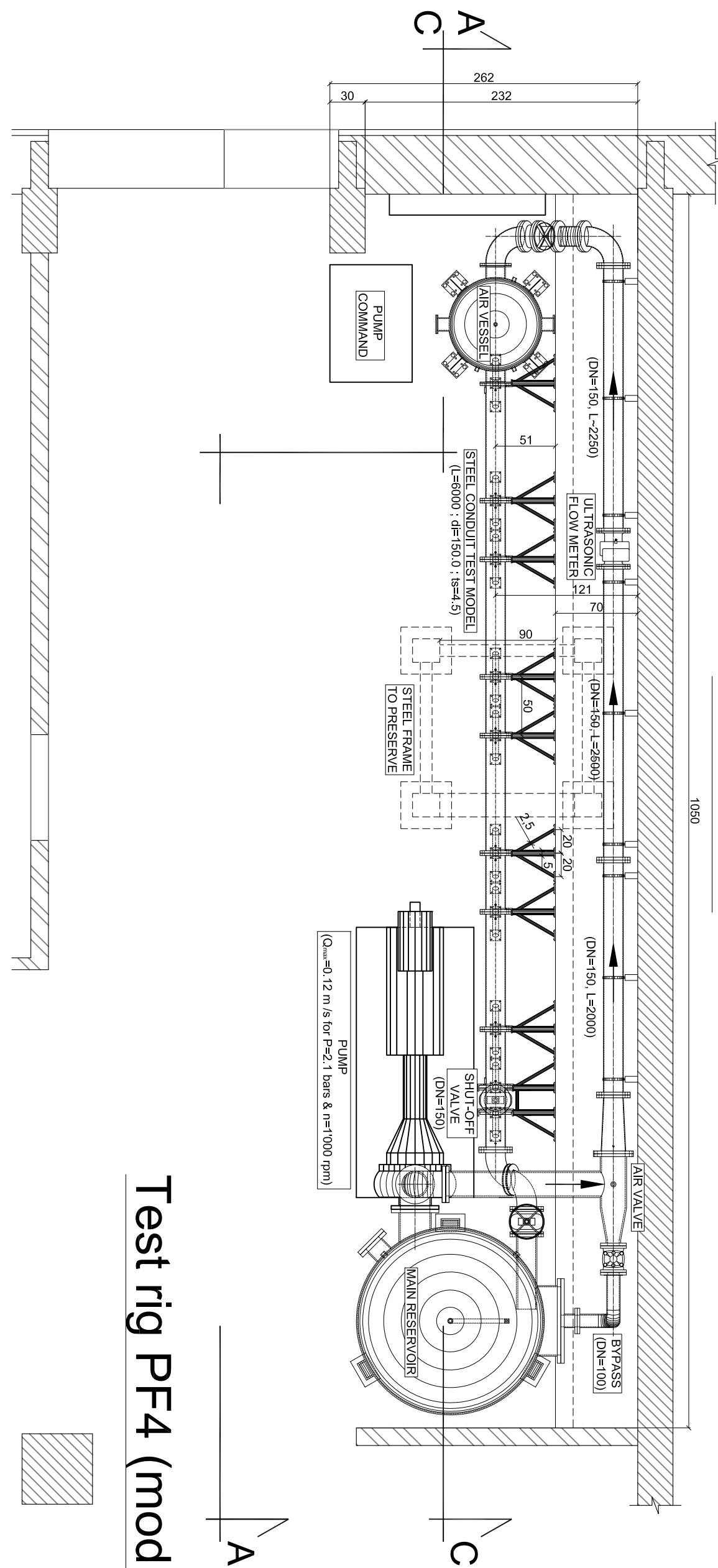
The construction drawings and test configurations of the physical scaled model

SECTION A-A (SCALE:1/10)

Test rig PF4 (modified state)

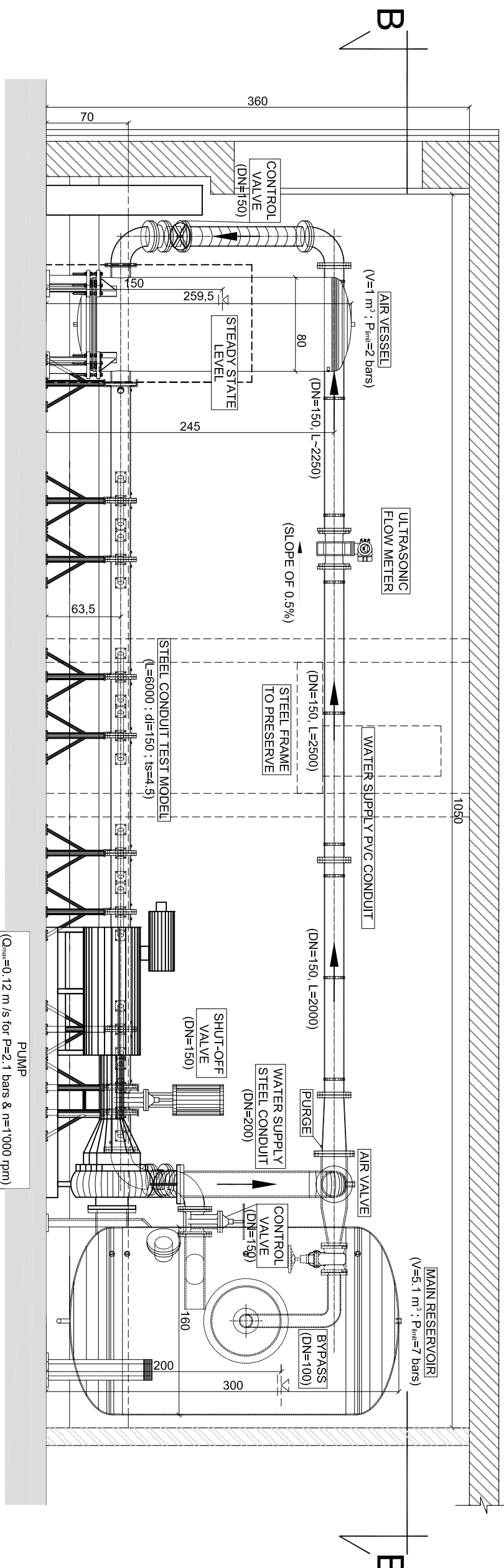
[1/2]

[1/2]

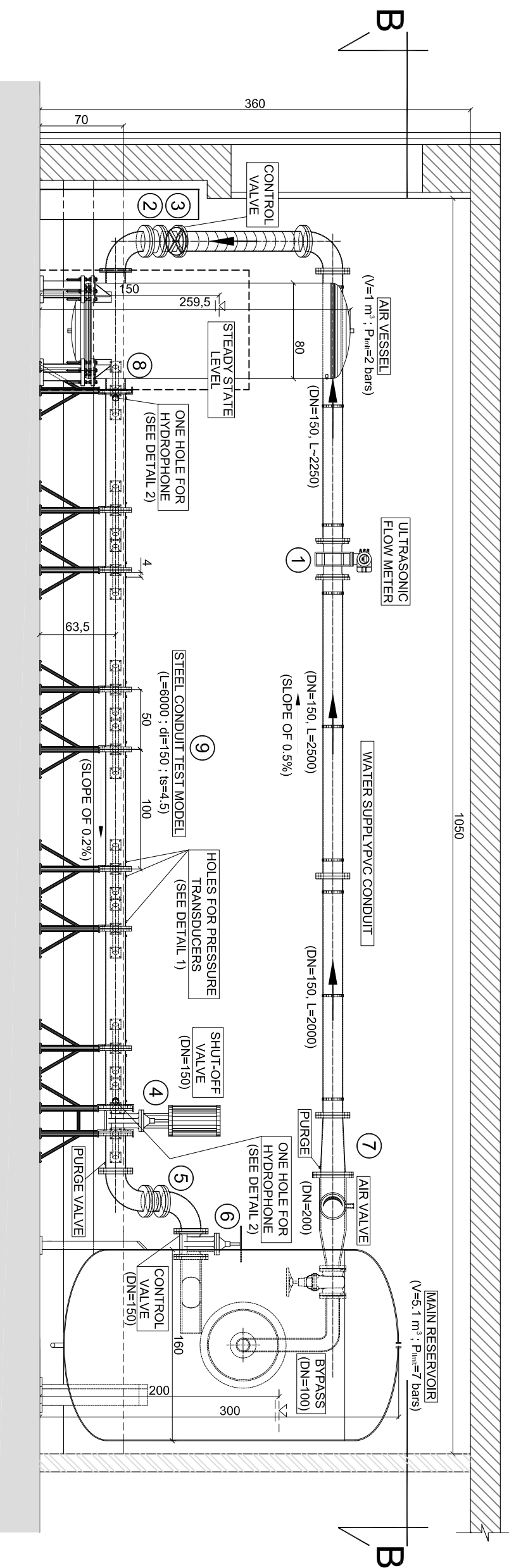


SECTION B-B (SCALE:1/10)

(Q_{max}=0.12 m/s for P=2.1 bars & n=1000 rpm)



SECTION C-C (SCALE:1/10)



NOTE 1

① FLOW METER, DN150, PN16

④ SHUT-OFF VALVE, DN150, PN10
(VONROLL, MODEL 5007)

② & ⑤ TUBOFLEX MODEL 5, DN150 PN16
(CONSTRUCTION LENGTH=100 TO 200 mm)

③ & ⑥ VALVE WITH FLANGES (VANNE A BRIDE)
DN150, PN16

⑦ ADAPTATION CONE, DN200-150, PN16

⑧ THE EXIT FROM THE AIR CHAMBER MUST BE ADAPTED
TO HAVE A CONDUIT CONNECTION OF AN INTERNAL
DIAMETER OF EXACTLY 150mm

⑨ THE INTERNAL DIAMETER OF THE TEST CONDUIT IS EQUAL
TO 150mm. FLANGES OF THIS CONDUIT ARE EQUIPPED
WITH AN "O-RING" JOINT TO FACILITATE THE CHANGE OF
CONDUIT PIECES ACCORDING TO THE TEST
CONFIGURATION

TYPICAL FLANGE DETAIL FOR PN10 & PN16

NOTE 2

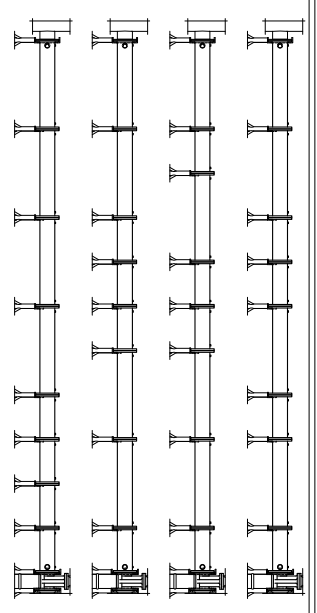
FOR DETAILS 1 AND 2, SEE MECHANICAL DETAIL DRAWING

NOTE: 1) THERE ARE FOUR CONDUIT PIECES OF 1m OF LENGTH AND FOUR CONDUIT PIECES OF 0.5m OF LENGTH
2) THE PIECE OF CONDUIT DOWNSTREAM VALVE IS FOR ADJUSTMENT, IT IS EQUIPPED WITH PURGE VALVE OF" 3) EACH PIECE OF THE TEST CONDUIT CONTAINS TWO HOLES FOR TRANSDUCERS PLACED AT 4cm FROM FLANGE'S FACE.

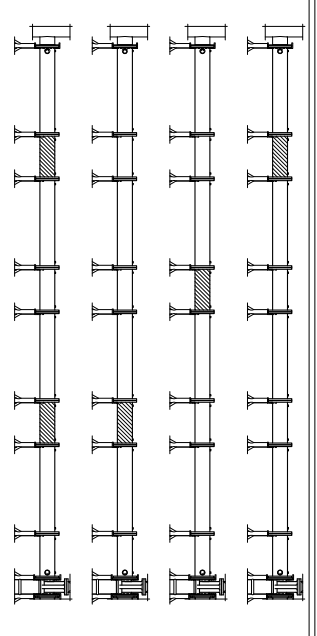
Test rig PF4 (modified state)

[2/2]

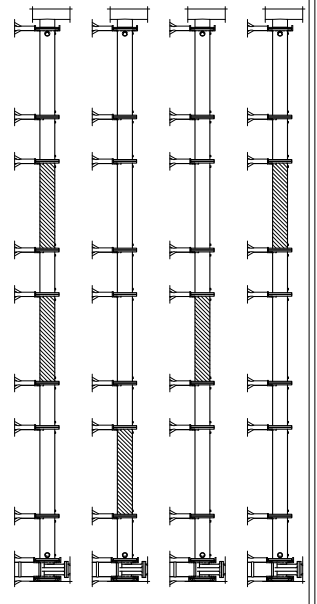
BASIC CONFIGURATION



LOCAL CHANGE OF RIGIDITY



CHANGE OF RIGIDITY OVER A CERTAIN DISTANCE



CHANGE OF RIGIDITY OVER A CERTAIN DISTANCE

STEEL (4 PIECES OF 50 cm AND 4 PIECES OF 100 cm OF LENGTH)

ALUMINIUM (3 PIECES OF 50 cm AND 3 PIECES OF 100 cm OF LENGTH)

PVC (3 PIECES OF 50 cm OF LENGTH)

INOX (3 PIECES OF 50 cm OF LENGTH AND 1 PIECE OF 100 cm)

QUANTITIES

STEEL

Article number 186.100.570; Debrunner,
 $a=159\text{mm}$; $t=4.5\text{mm}$; $L=600\text{cm}$

ALUMINIUM

Article number 114753; Metallica,
 $D=160\text{mm}$; $s=5.0\text{mm}$; $L=450\text{cm}$

PVC

Article number 4 ND; Notz, $\varnothing_{\text{ext.}}=160\text{cm}$;
 $TH=7.7\text{mm}$; $\varnothing_{\text{int.}}=144.6\text{cm}$; $L=150\text{cm}$

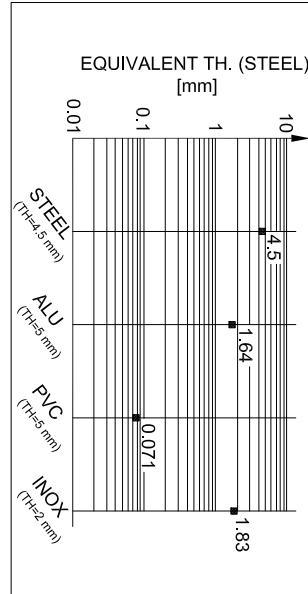
INOX

Article number 125512; Metallica; $L=250\text{cm}$;
 $D=154\text{mm}$; $d=150\text{mm}$; $s=2.0\text{mm}$

PHYSICAL PROPERTIES

	DENSITY [g/cm ³]	"E" MODULUS [MPa]
STEEL	7.85	210000
ALUMINIUM	2.70	69'000
PVC	1.40	3'000
INOX	8.03	193'000

EQUIVALENT THICKNESSES



43 COMBINATIONS
A TOTAL OF
43 COMBINATIONS

...

6 COMBINATIONS

6 COMBINATIONS

6 COMBINATIONS

6 COMBINATIONS

A.3

Sensing requirements for the prototype measurements

Sensing requirements for Grimsel II power plant

Task 7 of HYDRONET project

Pressurized shafts and tunnels

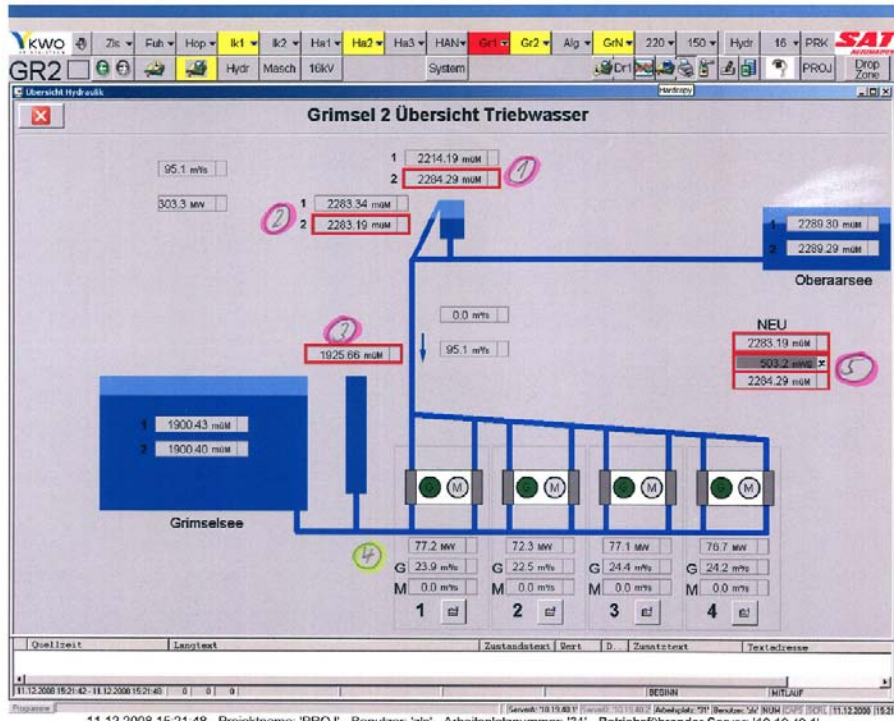
PhD researcher: Fadi Hachem

Lausanne, 30th June 2009

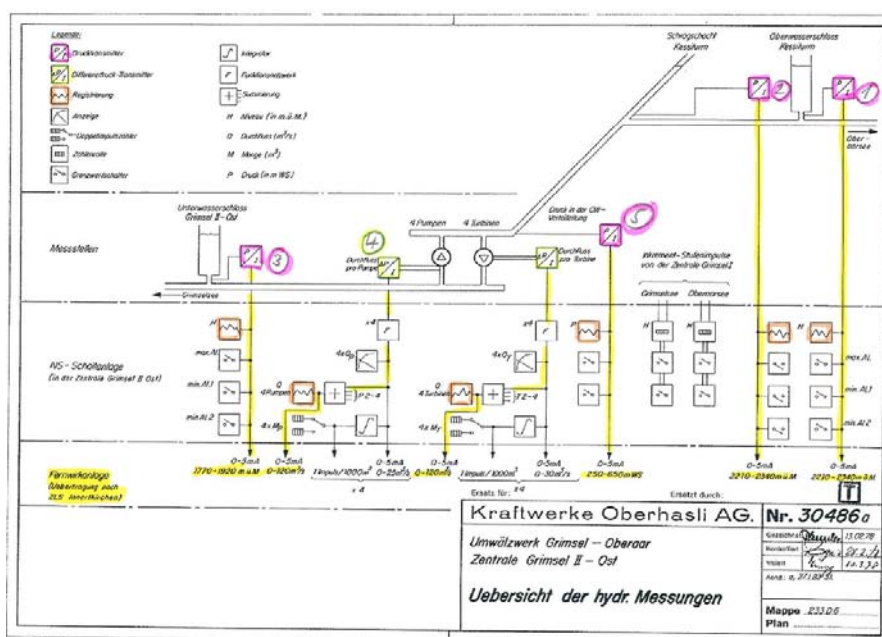
1- Existing sensors and measurement limitation

1.1 General measurement scheme

KWO communicated us (through Mr. Fankhauser) the disposition of the actually measured, transmitted and registered data in the Grimsel II power plant. The global measurement scheme is shown on Figures 2.a & 2.b.



(a)



(b)

Figure 2: Global scheme and locations of the actual measured data

1.2 Pressure and water level measurements

Pressure data registered at points 1, 2, 3 and 5 can be transmitted to *Innertkirchen* acquisition centre and then to us on demand by Mr. Winkler.

After receiving and analyzing some data, we can consider that:

- The water level measurements inside the vertical surge tank (point 1) and inside the inclined shaft in the Kessiturm (point 2) are valid to detect water mass oscillation and the mean upstream water pressure in the pressurized shaft (Figure 3). Nevertheless, sensors equipping these positions do not have sufficient measuring frequency (limited to 1 Hz) to detect water hammer pulsation and therefore, **additional pressure sensors are needed upstream the pressurized shaft**.
- The pressure measured at the downstream end of the shaft (point 5) does not have the required frequency to measure the water hammer transient (Figure 4). So, **additional pressure sensors are also needed downstream the pressurized shaft**.
- Data acquired from point 3 are not needed now because, from a pressure point of view, we are interested only in what is happening on the high pressure side of the Grimsel II power plant.

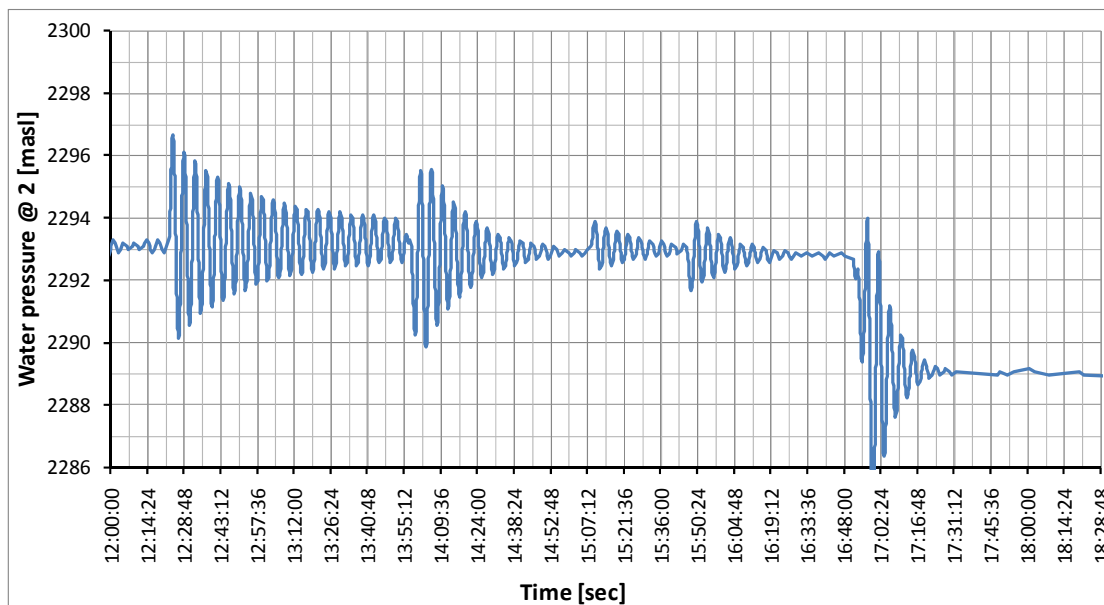


Figure 3: Water level variation in time inside the *Schrägschacht* upstream the pressurized shaft (same data are also available for point 1)

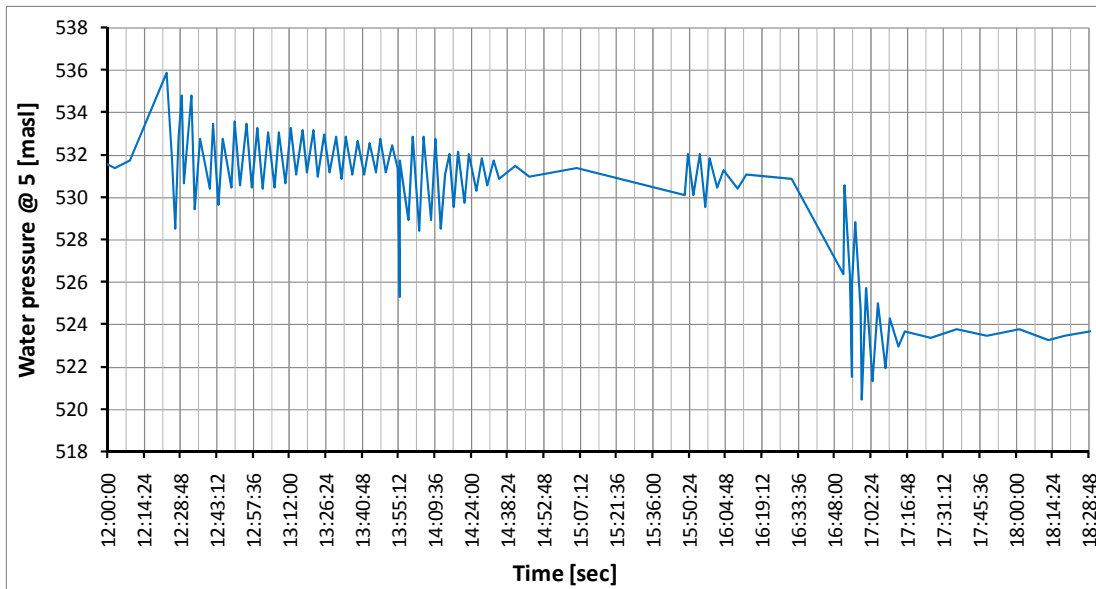


Figure 4: Water pressure variation in time at the downstream end of the pressurized shaft (data at point 5)

1.3 Water flow measurements

The water flow of each turbine or pump is actually available from measurements done on points 4. A specimen of these flow measurements is shown on Figure 5. They can be considered as sufficient for us and **no additional water flow sensors are needed.**

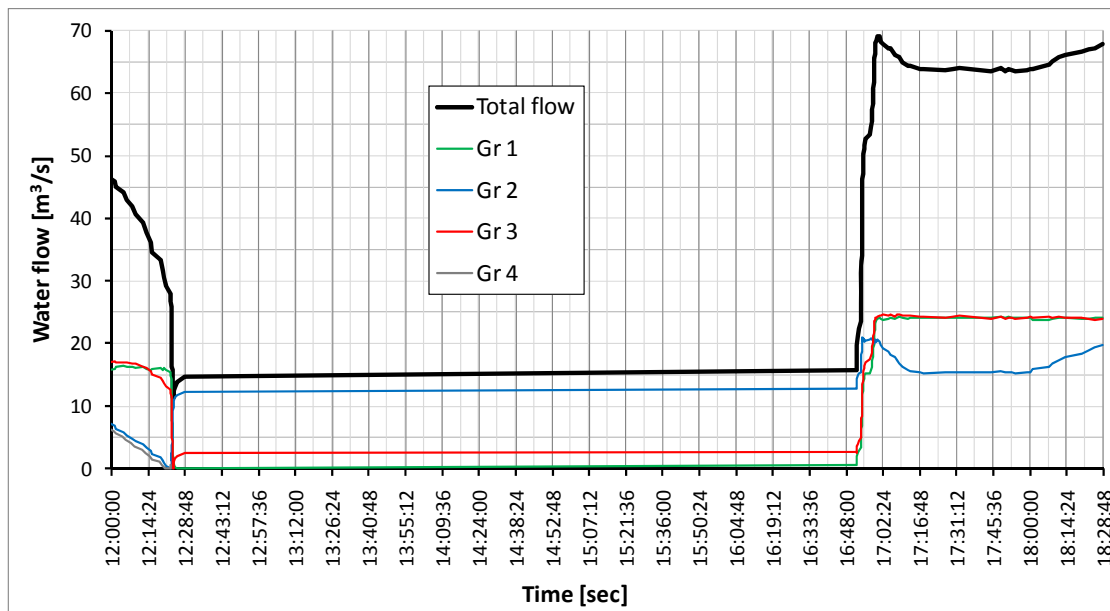


Figure 5: Water flow variations in time measured at each turbine or pump (data at points 4)

2- Additional sensors needed (type and location)

2.1 Pressure transducers

Type: Kistler, 4045A100.

Remarks: the head of the pressure sensors must be in contact with water inside the main shaft. If we put these sensors in by-passes far from the shaft we risk losing dynamic signals.

Locations: Two locations are needed to place pressure sensors (one sensor in each location). The first location is at the upstream end of the pressurized shaft (Figures 6.a & 6.b) and the second one is at the shaft entrance into the power house (Figures 7.a, 7.b and 7.c).

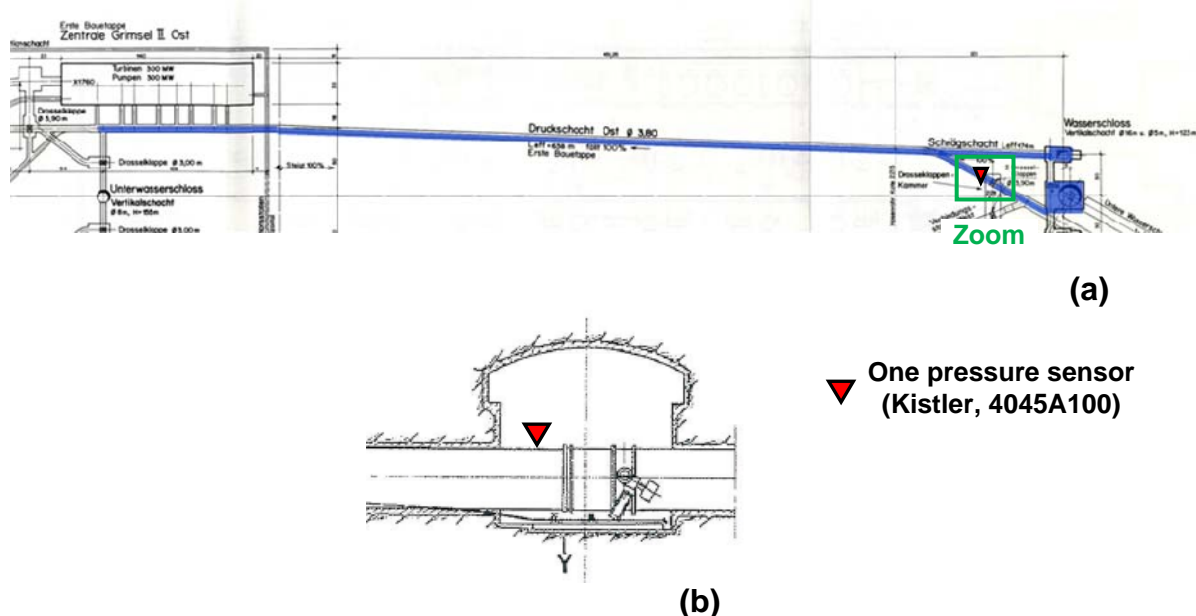
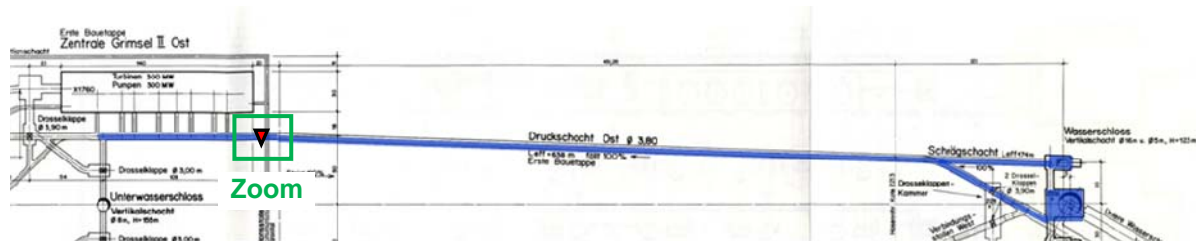
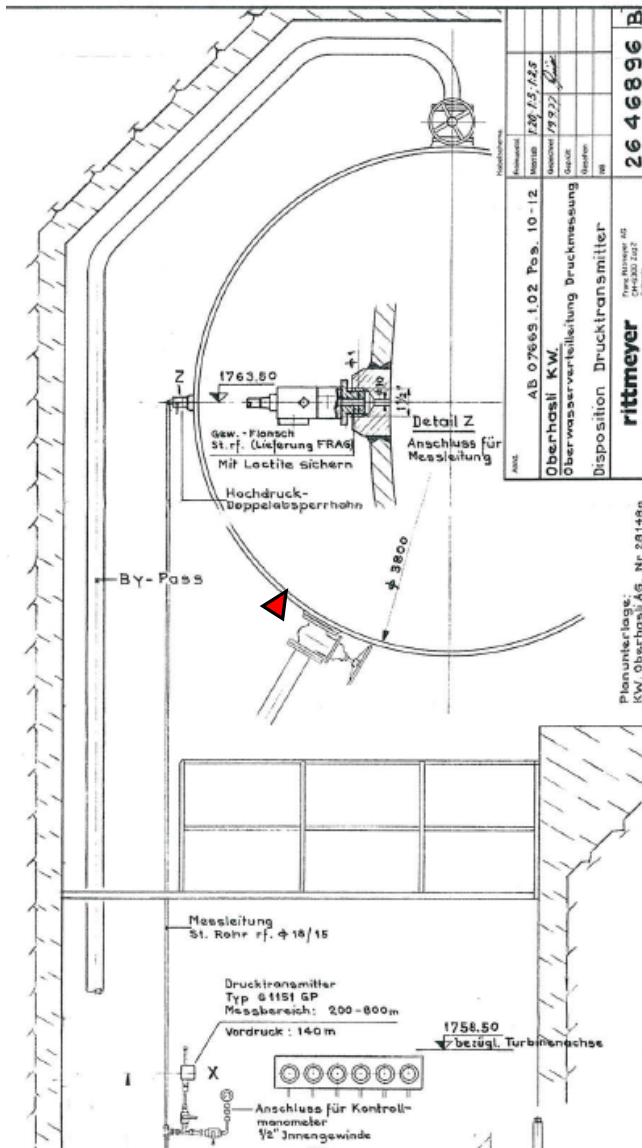


Figure 6: Pressure sensor location at the upstream side of the shaft

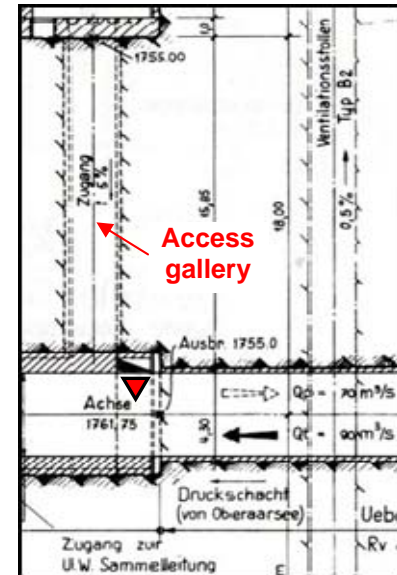
- (a) Plan view of the high pressure side of Grimsel II power plant
- (b) Elevation zoom inside the gallery of the security shut-off valve where the pressure sensor will be placed on the main shaft in contact with water



(a)



(b)



(c)

One pressure sensor
(Kistler, 4045A100)

Figure 7: Pressure sensor location at the downstream side of the shaft

- Plan view of the high pressure side of Grimsel II power plant
- Elevation zoom inside the gallery where the pressure sensor will be placed on the main shaft
- Plan view zoom of the access gallery and sensor location

2.2 Geophones sensors

Type: Sensor Nederland, SM-6/U-B 4.5 Hz.

Remarks: Geophone sensors are capable of measuring the velocity of the vibrating motion propagating inside materials.

Locations: Three locations are needed to place geophone sensors (one sensor in each location). The first location is at the upstream end of the pressurized shaft (Figures 8.a & 8.b), the second one is at the shaft entrance into the power house (Figures 9.a and 9.b) and the third location is inside the ventilation gallery that passes above the high pressure side of the shaft (Figures 10.a, 10.b & 10.c).

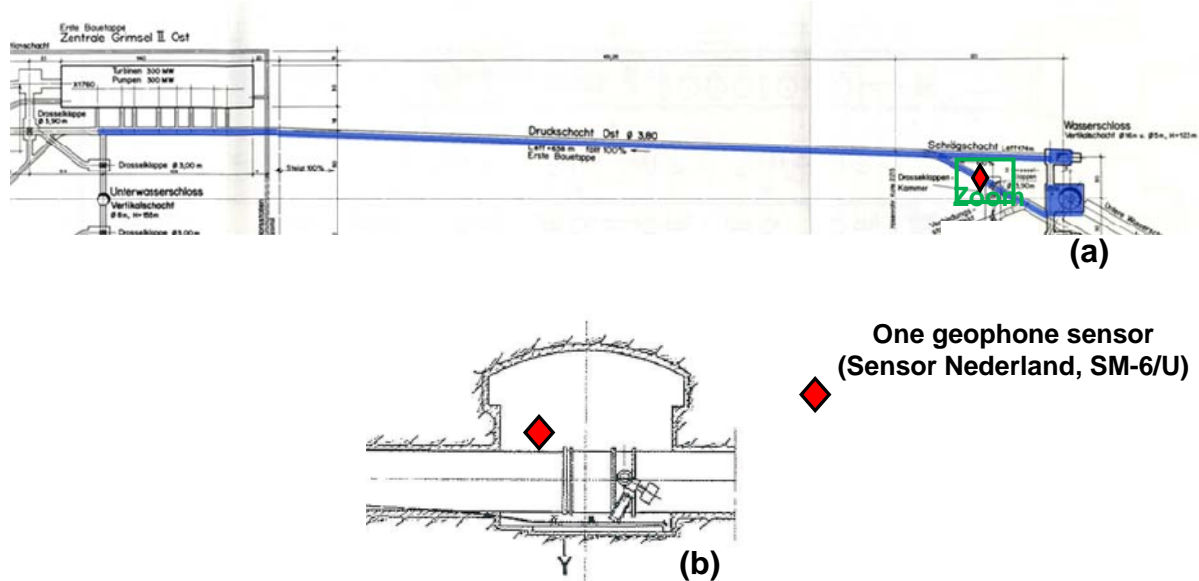
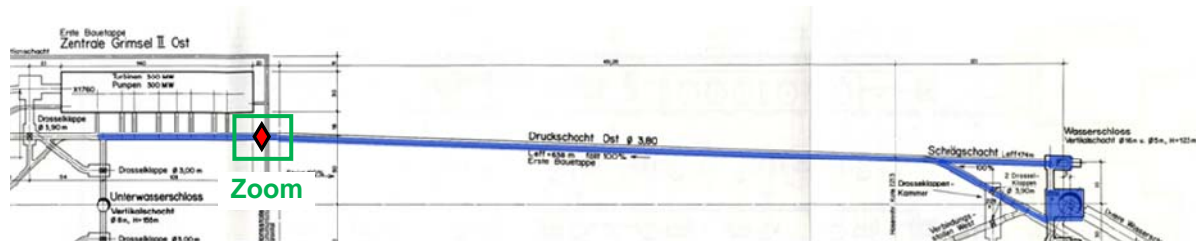
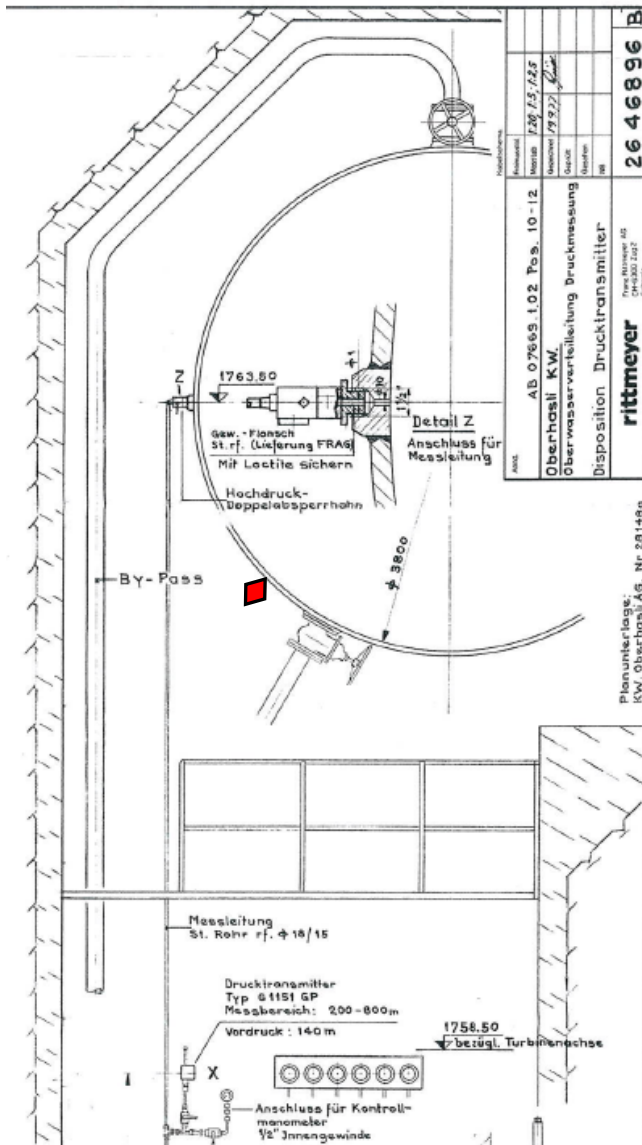


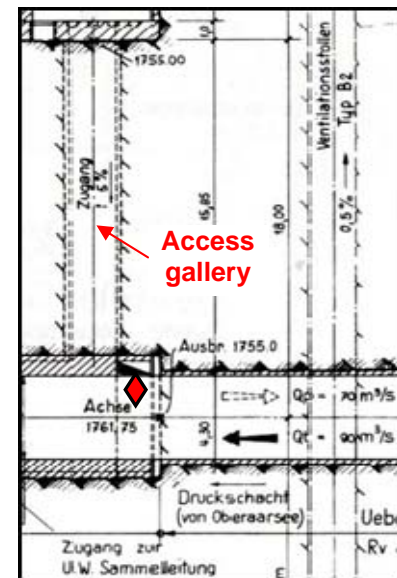
Figure 8: Geophone sensor location at the upstream side of the shaft
 (a) Plan view of the high pressure side of Grimsel II power plant
 (b) Elevation zoom inside the gallery of the security shut-off valve where the geophone sensor is placed on the steel of the main shaft



(a)



(b)



(c)

Figure 9: Geophone sensor location at the downstream side of the shaft

- Plan view of the high pressure side of Grimsel II power plant
- Elevation zoom inside the gallery where the geophone sensor is placed in contact with the steel of the main shaft
- Plan view zoom of the access gallery and sensor location

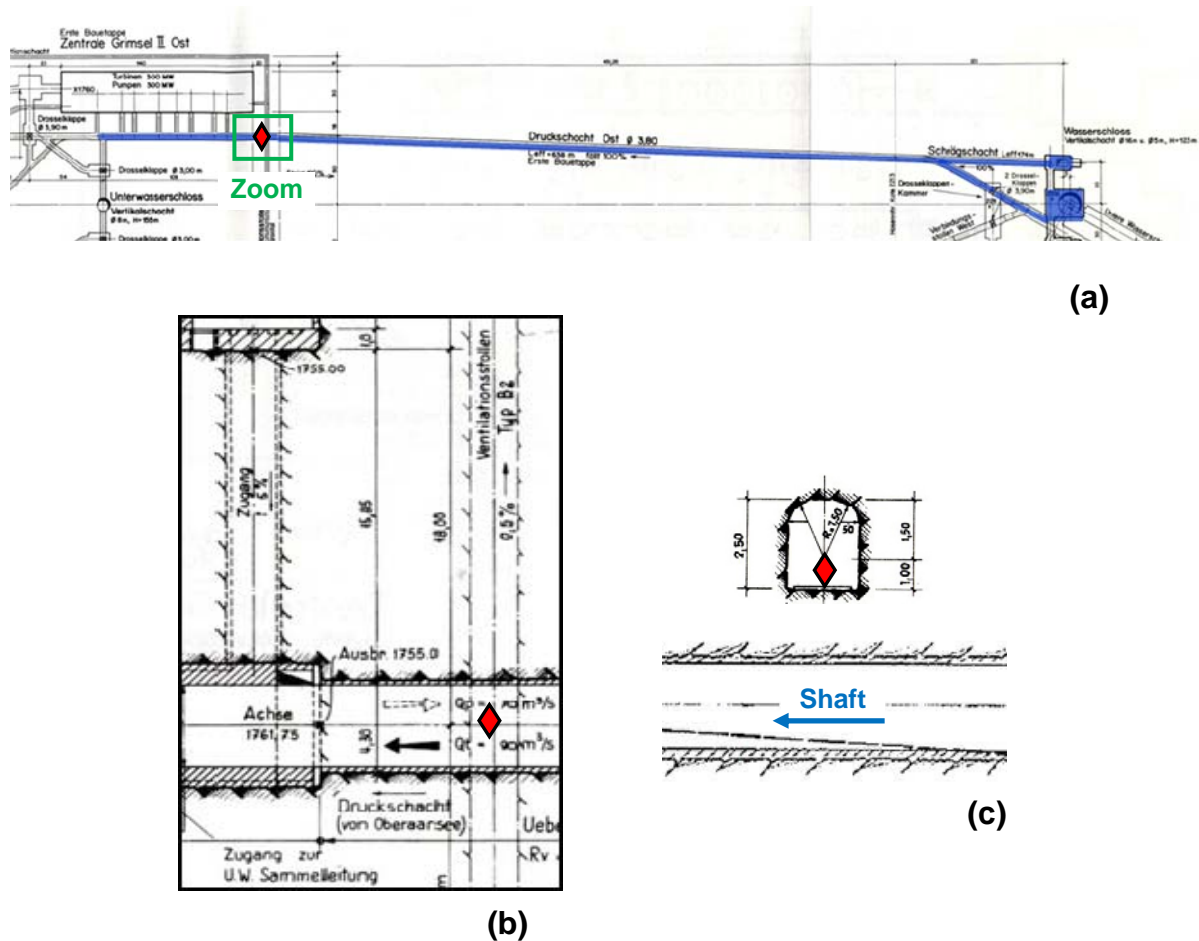


Figure 10: Geophone sensor location at the downstream side of the shaft in the ventilation gallery

- (a) Plan view of the high pressure side of Grimsel II power plant
- (b) Plan view zoom inside of the ventilation gallery above the shaft where the geophone sensor is place in contact with rock
- (c) Section of the ventilation gallery above the shaft

2.3 Hydrophones sensors

Type: Cetacean Research Technology, CR1 hydrophone.

Remarks: Hydrophone sensors measure acoustic pressure (or small pressure variations) inside water. They are much more sensitive from pressure transducers and need to be in contact with water.

Locations: Three locations are needed to place hydrophone sensors (one hydrophone in each location). The first location is into the inclined shaft (Figures 11.a & 11.b), the second one is inside the main shaft near the security shut-off valve (Figures 12.a & 12.b) and the third position is inside the shaft at the entrance into the power house (Figures 13.a & 13.b).

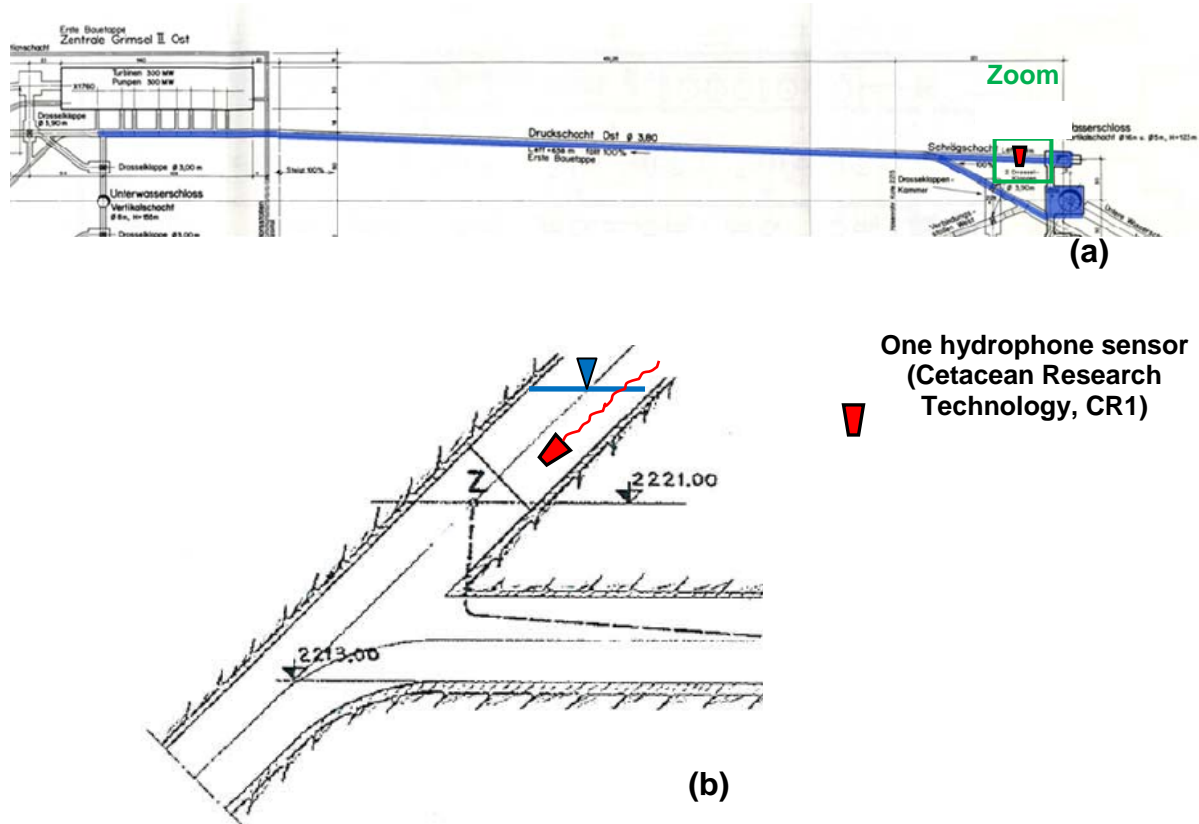


Figure 11: Hydrophone sensor location at the upstream side of the shaft
 (a) Plan view of the high pressure side of Grimsel II power plant
 (b) Elevation zoom inside the inclined shaft where the hydrophone sensor is slipped into water from above

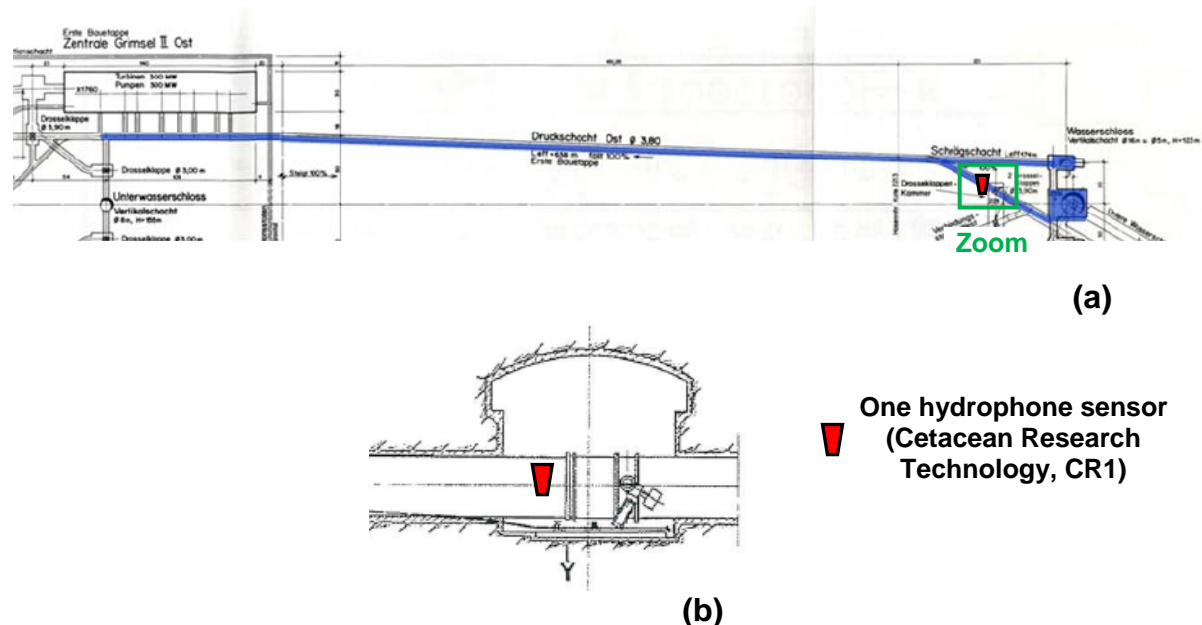
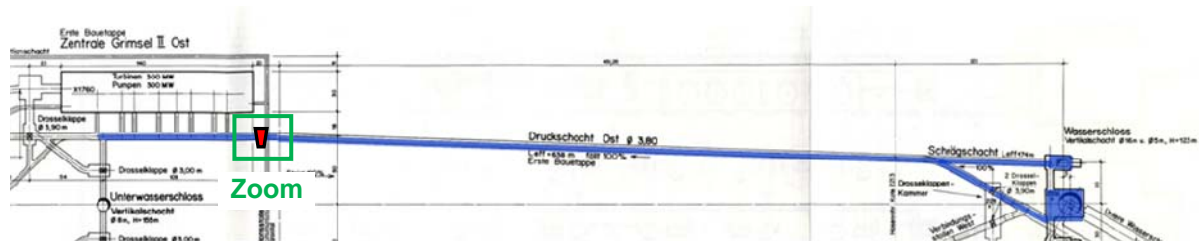
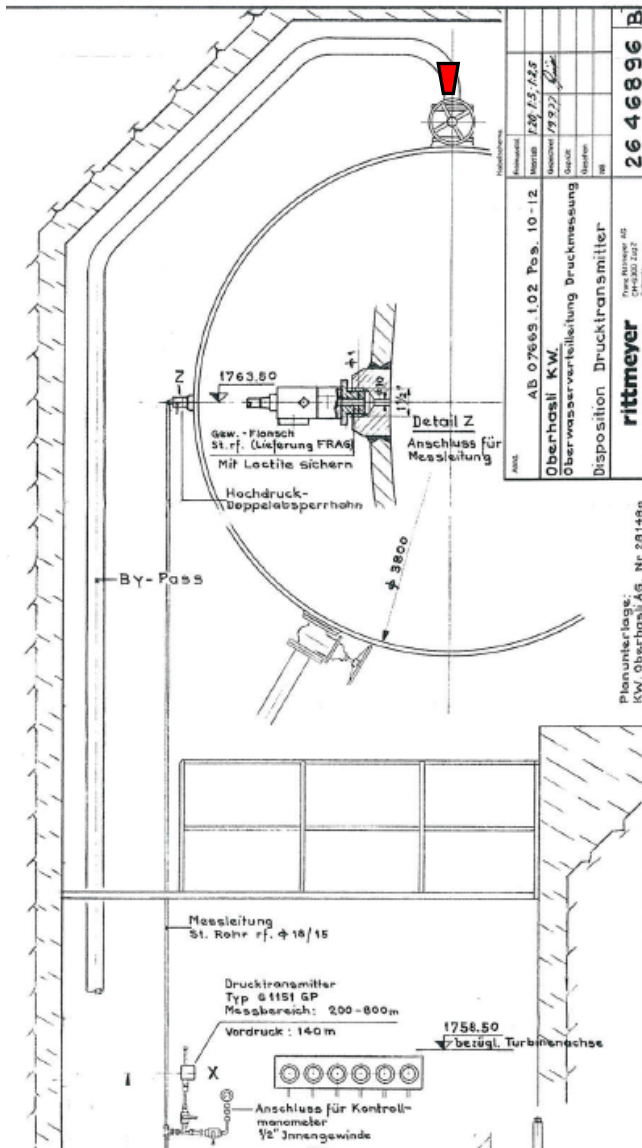


Figure 12: Hydrophone sensor location at the upstream side of the shaft

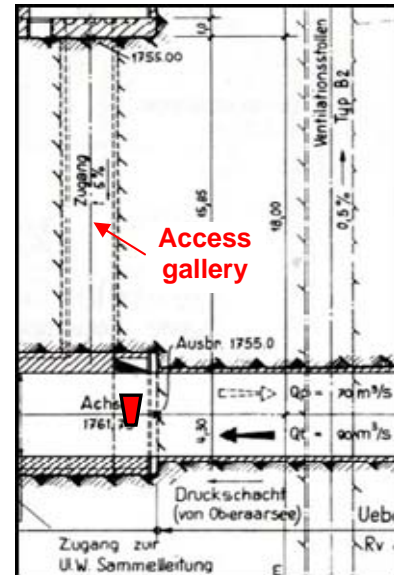
- (a) Plan view of the high pressure side of Grimsel II power plant
- (b) Elevation zoom inside the gallery of the security shut-off valve where the hydrophone sensor is placed inside water at a certain by-pass (if any) of the main shaft



(a)



(b)



(c)

Figure 13: Hydrophone sensor location at the downstream side of the shaft

- (a) Plan view of the high pressure side of Grimsel II power plant
- (b) Elevation zoom inside the gallery where the hydrophone sensor is placed in contact with water in the upper by-pass of the shaft
- (c) Plan view zoom of the access gallery and sensor location

3- Data acquisition and data storage locations

Data acquisition involves gathering signals from measurement sensors (using cables), digitizing the signal for storage (using an acquisition card) and storage, analysing and presenting digitized signal on a PC.

Locations: Three data acquisition locations and storage are needed to gather the data acquired from the different sensors used. Electricity is required at each of the acquisition position.

At the upstream end of the shaft, the first location is inside the gallery of the security shut-off valve at level 2'211 masl (Drosselklappen-Kammer) while the second location is on the surge tank plat-form at level 2'336 masl (Figure 14).

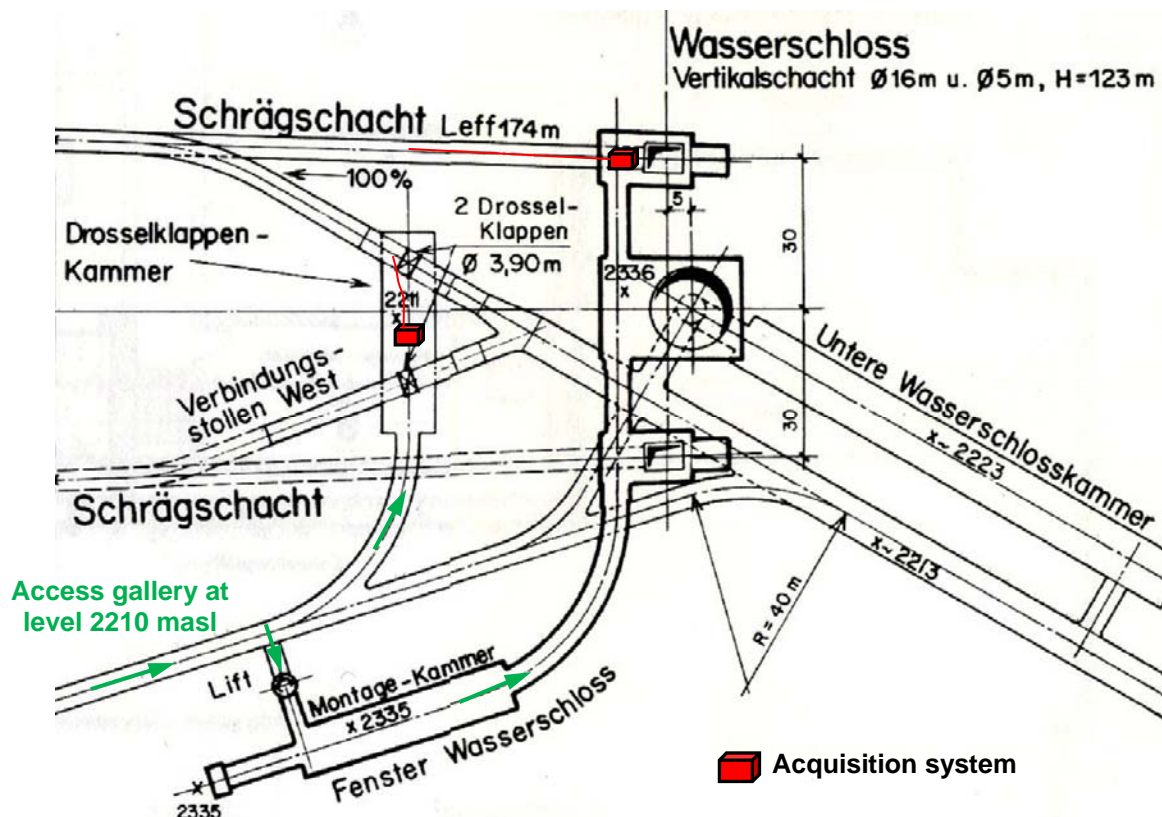
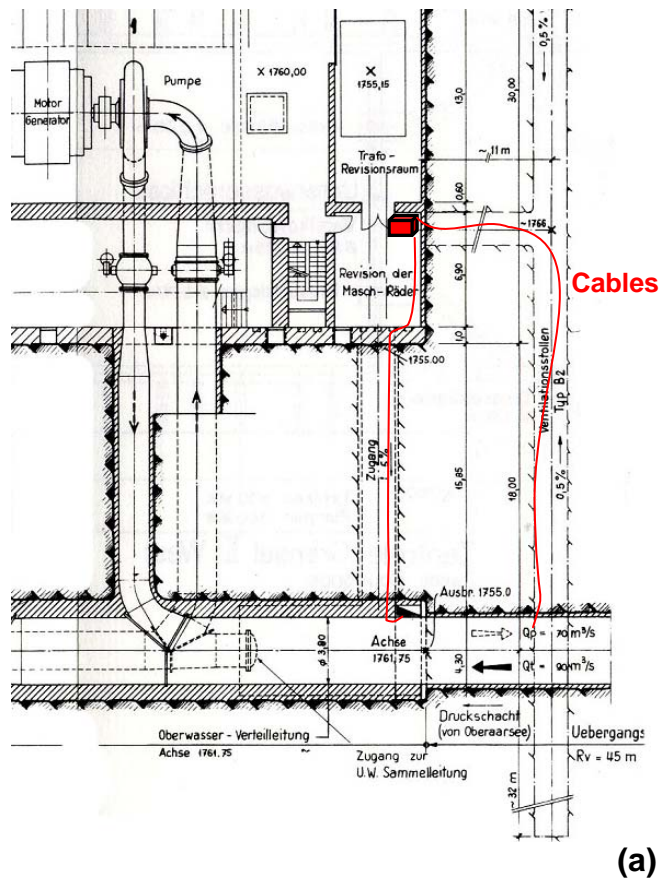
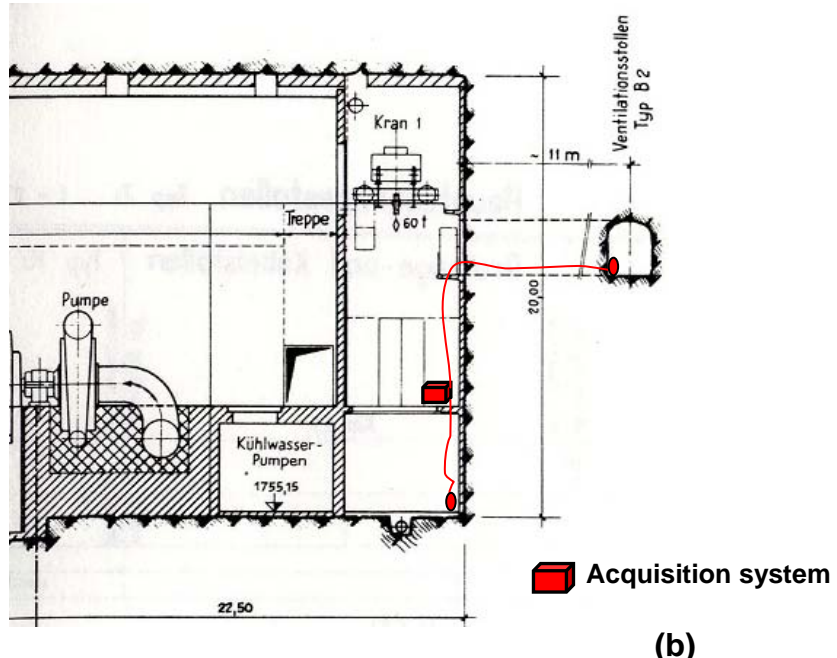


Figure 14: Data acquisition and storage locations at the upstream end of the shaft

At the downstream end of the shaft, the third acquisition location is inside the power house at level 1'760 masl (Figures 15.a & 15.b).



(a)



(b)

Figure 15: Data acquisition and storage locations at the downstream end of the shaft (in the power house)
 (a) Plan view; (b) Section